

Hybrid simulation with multiple actuators: a state-of-the-art review

Amirali Najafi^a, Gaston A. Fermandois^{b,*}, Shirley J. Dyke^c, and Billie F. Spencer, Jr.^d

^aCenter for Advanced Infrastructure and Transportation, Rutgers University, Piscataway, NJ, USA

^b Departamento de Obras Civiles, Universidad Técnica Federico Santa María, Santiago, Chile

^c*School of Mechanical Engineering, Purdue University, West Lafayette, IN, USA*

^d*Department of Civil and Environmental Engineering, University of Illinois at Urbana-Champaign, Urbana, IL, USA*

*Correspondence: gaston.fermandois@usm.cl

Abstract

This paper reviews the conceptual and technical advances in multi-actuator dynamic loading in modern structural testing. In particular, a focus is given to the developments and challenges in multi-axial hybrid simulation (maHS) and multi-axial real-time hybrid simulation (maRTHS), where a specimen is subjected to multi-directional dynamic loading by interacting with a numerical simulation of its surrounding structural subsystems and components. This review introduces the general framework for maHS and maRTHS, describing substructuring techniques, loading equipment, and nonlinear kinematics. In particular, the process of dynamic compensation for multi-actuator loading assemblies in maRTHS is explored. Different compensation architectures in the task (Cartesian) and joint (actuator) spaces are covered, and each alternative is assessed on its own merits for dynamic synchronization of multi-actuator loading platforms. Finally, current challenges in maHS and maRTHS testing are identified, with recommendations for future research endeavors for the scientific community.

Keywords: Hybrid simulation; structural testing; substructuring; multiple actuators; non-linear kinematics; specimen-actuator interaction; dynamic compensation.

27 **Contents**

28	1 Introduction	3
29	2 General framework for multi-actuator loading	5
30	2.1 Substructuring for hybrid testing	5
31	2.2 Tracking algorithms in multi-actuator hybrid simulation	11
32	2.3 Kinematics of multi-actuator loading assemblies	13
33	3 Structural testing with multi-actuator devices	16
34	3.1 Shake tables	16
35	3.2 Boundary condition devices	17
36	3.3 Shell element testers	18
37	3.4 Individually attached actuators	18
38	4 Multi-axial hybrid simulation (maHS)	19
39	4.1 Multi-actuator applications	19
40	4.2 Multi-axial applications	20
41	5 Multi-axial real-time hybrid simulation (maRTHS)	21
42	5.1 Multi-actuator applications	21
43	5.2 Multi-axial applications	23
44	5.3 Multi-axial real-time testing in other engineering disciplines	24
45	6 Current challenges and opportunities	25
46	6.1 Robustness of multi-actuator closed-loop systems	25
47	6.2 Mechanical design of multi-actuator loading assemblies	26
48	6.3 Time constraints and computational efforts	27
49	6.4 Validation of multi-actuator RTHS	27
50	6.5 Other applications regarding multi-axial testing	28
51	7 Concluding remarks	28

52 **Terminology**

53	Boundary conditions physical interfaces between experimental and numerical substructures
54	enforced by actuators.
55	Actuator compensation algorithm intended to minimize the synchronization error between
56	target and measurement signals from an actuator.
57	Coupled compensation every actuator's control signal is determined by feedback from all
58	other actuators. Also known as centralized or multi-input multi-output (MIMO) compensation.
59	

60 **Decoupled compensation** every actuator's control signal is determined by feedback from
61 itself. Also known as decentralized or single-input single-output (SISO) compensation.

62 **Parallel manipulator** actuated system where the ends of all actuators are connected to a
63 rigid platform, creating a kinematic loop.

64 **Substructuring** process of simulating the dynamics of a mechanical system by means of ana-
65 lyzing the sum of its constituents.

66 1 Introduction

67 Experimental testing is a fundamental step in the development of innovative, sustainable, and
68 reliable materials and structural systems. The predominant structural test methods employed
69 have been: (1) quasi-static testing, where a cyclic trajectory often with increasing amplitude
70 is imposed at slow (i.e., near static) speeds on a physical specimen to identify the nonlinear
71 hysteretic behaviors under load reversals; (2) shake table testing, for identifying the behavior
72 of a complete structure through the application of base motion; and (3) hybrid simulation (also
73 called pseudo-dynamic testing, dynamic virtualization, and hardware-in-the-loop testing), where
74 the behavior of a complete structure is simulated via the interaction of numerical modeling and
75 experimental testing [1, 2].

76 The response of a structural component is a function of the loading history it has experienced
77 and the boundary conditions with the greater structural system. Thus, hybrid simulation (HS)
78 was proposed as an alternative to quasi-static testing, which is capable of incorporating system-
79 level interactions with realistic excitations [3, 4, 5, 6]. HS is a versatile methodology that
80 addresses many of the limitations with other test methods. For example, quasi-static testing
81 often employs simplistic cyclic trajectories which are not entirely representative of the behaviors
82 experienced by a structural element under environmental loading. Also, shake table testing is
83 limited by the equipment available to test an entire floor plan with a base excitation. Shake
84 tables have size and payload limitations, and often the consequence is testing of scaled structures.
85 With HS, only the structural elements of interest are experimentally tested and the excitation
86 can be applied with more flexibility through different actuator configurations. Although size
87 and capacity limitations continue to exist with HS, a wider range of experiments are possible
88 in a wider range of labs.

89 Real-time hybrid simulation (RTHS) is a variation of hybrid simulation, where the sim-
90 ulation has real-time constraints, thus enabling the study of physical specimens with rate-
91 91 dependent behaviors [7]. Whether or not real-time testing is possible depends on the avail-
92 ability of dynamically-rated actuators and real-time computational resources. Servo-hydraulic
93 actuators saw vast growth due to the need to simulate realistic flight conditions with the onset
94 of the space age in the 1950s and 1960s [8]. At that time, dynamic structural testing became
95 possible due to improvements in servo-valve technology, higher flow capacity, resonant load
96 stabilization, and static compensation for structural compliance [9]. The exponential growth
97 in computational capabilities combined with the diminishing costs also played a critical role in
98 realizing the first RTHS tests in the 90s and various more sophisticated implementations since
99 [10].

100 The choice between slow speed and real-time tests also depends on the rate-dependence of
101 the materials and structures under consideration, the natural frequency of the structure, and
102 the characteristics of the structural loading. For instance, a stiff structure (i.e, having large
103 natural frequencies) and an excitation with a high frequency content may experience strain-rate
104 induced increases in capacity. Some studies have explored the dependence of common building
105 materials (e.g., steel and concrete) to the rate of loading [11, 12, 13]. Many studies have reported
106 negligible rate-dependent findings in common structural materials [14, 15, 16]. The discussion
107 on the need for real-time testing of common building materials is not settled. Nonetheless,
108 dampers, isolation systems, and many modern materials are rate-dependent [17, 18].

109 Other external factors may influence the consideration between HS and RTHS. In the hybrid
110 fire test conducted by [19], strain rate is not high but the rate of temperature increase is quite
111 rapid. Therefore, the experiment had to be conducted in real-time to ensure the temperature
112 gradient in the physical specimen is realistic.

113 Hybrid simulation researchers have considered many extensions to the original technique,
114 including the use of multiple actuators in conjunction for higher loading capacity and to pre-
115 scribe displacements over a physical specimen at more than one degree-of-freedom (DOF). The
116 authors have identified several literature reviews pertaining to these expansions which discuss
117 the general framework of slow speed and real-time methodologies and the variants of the dy-
118 namic substructuring concept [20, 21, 22, 23, 24, 25]. However, a review of the developments
119 with multiple actuators coupled through a continuum body was not identified.

120 This review article provides an updated perspective on the various contributions in HS and

121 RTHS with multi-actuator loading. In Section 2, a general framework for multi-actuator hybrid
 122 simulation is described including developments made in actuator compensation and kinematic
 123 transformations. In Section 3, noteworthy classes of multi-actuator devices for structural testing
 124 are listed, including shake tables, boundary condition devices, and shell element testers. Section
 125 4 and 5 are devoted to developments in multi-axial hybrid simulation (maHS) and multi-axial
 126 real-time hybrid simulation (maRTHS), respectively. Section 5 describes multi-actuator RTHS
 127 developments which operate in single-axis configurations. Lastly, Section 6 highlights many
 128 of the current challenges with multi-actuator loading and suggests research avenues for the
 129 maHS/maRTHS community to explore.

130 **2 General framework for multi-actuator loading**

131 In this section, the general framework and technical prerequisites for multi-actuator HS and
 132 RTHS are discussed, and the two variations are distinguished from one another. The procedure
 133 for maHS and maRTHS can be simplified into four tasks: (1) simulation of the numerical
 134 substructure subject to external loading (e.g., ground motion); (2) imposition of displacements
 135 and forces at the boundary interface between the numerical and experimental substructures
 136 through a multi-actuator loading assembly; (3) direct measurement of experimental substructure
 137 response; and (4) feedback of measured experimental responses to the numerical substructure to
 138 close the hybrid simulation loop. The framework discussed herein is the foundation upon which
 139 many of the developments in multi-actuator hybrid simulation rest, and will help in explaining
 140 many of the references discussed in this review.

141 **2.1 Substructuring for hybrid testing**

142 Consider a system of second-order differential equations (i.e., equation of motion, EOM) used
 143 to represent the dynamics of a reference structure in a domain Ω :

$$\Omega : \quad \mathbf{M}\ddot{\mathbf{x}}(t) + \mathbf{C}\dot{\mathbf{x}}(t) + \mathbf{R}(\mathbf{x}, \dot{\mathbf{x}}) = \mathbf{p}(t) \quad (1)$$

144 where the vectors $\mathbf{x}(t) \in \mathbb{R}^n$, $\dot{\mathbf{x}}(t) \in \mathbb{R}^n$, and $\ddot{\mathbf{x}}(t) \in \mathbb{R}^n$ represent the displacement, velocity,
 145 and acceleration vectors relative to the ground floor, respectively. $\mathbf{M} \in \mathbb{R}^{n \times n}$ and $\mathbf{C} \in \mathbb{R}^{n \times n}$
 146 are the mass and damping matrices, respectively. The damping matrix is representative of the
 147 various frictional and dissipative mechanisms that exist in structures. Because damping is a

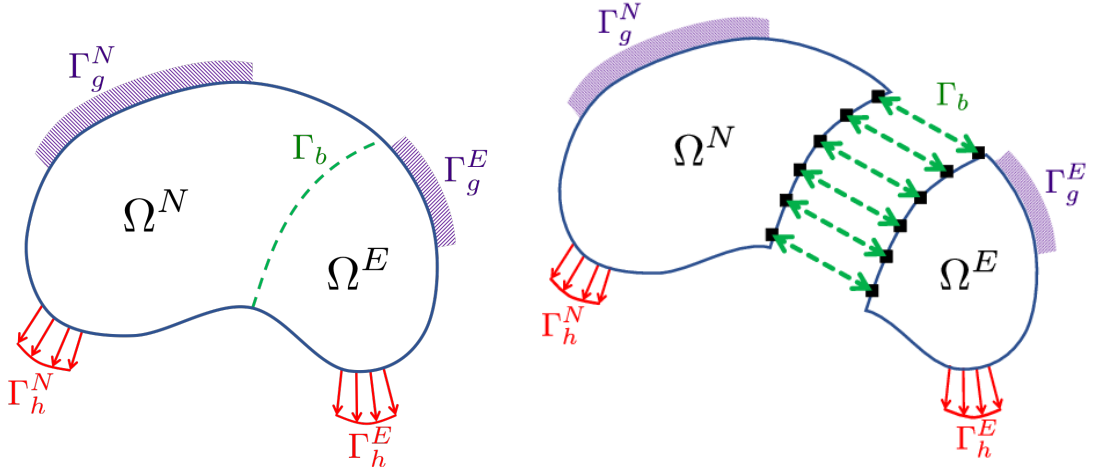


Figure 1: Substructuring of dynamical system

148 difficult phenomenon to model, it is customary to assume the damping matrix as proportional
 149 to the mass and stiffness matrices [26]. $\mathbf{R}(\mathbf{x}, \dot{\mathbf{x}}) \in \mathbb{R}^n$ is the vector of restoring forces, which is
 150 as a function of states $\{\mathbf{x}, \dot{\mathbf{x}}\}$. Finally, $\mathbf{p}(t) \in \mathbb{R}^n$ is the total load vector. Note that the time t
 151 is the load time, while the hybrid testing process may actually occur on an extended time scale.

152 Instead of solving the equations pertaining to the entire reference structure, a process known
 153 as *substructuring* is performed to subdivide it into smaller substructures, shown in Fig. 1.
 154 These equations can be solved independently, provided that the coupling between components
 155 is enforced by means of compatibility and equilibrium conditions at their boundary conditions
 156 [20, 27]. Then, a reference structure can be defined as the union of the two smaller substructures,
 157 $\Omega = \Omega^N \cup \Omega^E$, where Ω^N and Ω^E are the domains of numerical and experimental substructures,
 158 respectively. Each substructure has its own DOFs and boundaries. Let the displacement vector
 159 of the associated numerical and experimental substructures be defined as:

$$\mathbf{x}^N = \begin{Bmatrix} \mathbf{x}_i^N \\ \mathbf{x}_b^N \end{Bmatrix}, \quad \mathbf{x}^E = \begin{Bmatrix} \mathbf{x}_i^E \\ \mathbf{x}_b^E \end{Bmatrix} \quad (2)$$

160 where the superscripts N and E refer to the numerical and experimental substructures, respec-
 161 tively; and subscripts i and b refer to the interior and boundary DOFs, respectively, as shown
 162 in Fig. 2.

163 Then, the coupled EOM for both numerical and experimental substructures are expressed
 164 as follows:

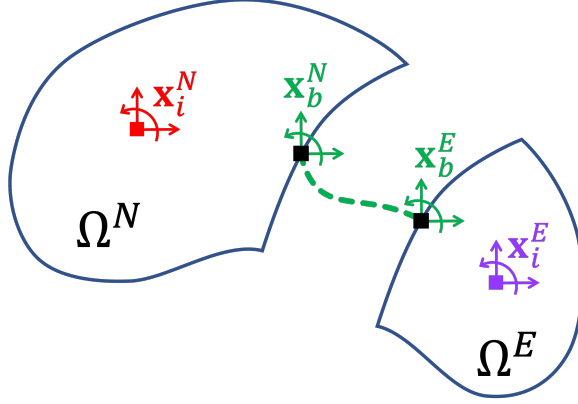


Figure 2: Degrees-of-freedom (DOF) of numerical (Ω^N) and experimental (Ω^E) substructures

$$\Omega^N : \quad \mathbf{M}^N \ddot{\mathbf{x}}^N + \mathbf{C}^N \dot{\mathbf{x}}^N + \mathbf{R}^N(\mathbf{x}^N, \dot{\mathbf{x}}^N) = \mathbf{p}^N + \mathbf{g}^N \quad (3)$$

$$\Omega^E : \quad \mathbf{M}^E \ddot{\mathbf{x}}^E + \mathbf{C}^E \dot{\mathbf{x}}^E + \mathbf{R}^E(\mathbf{x}^E, \dot{\mathbf{x}}^E) = \mathbf{p}^E + \mathbf{g}^E \quad (4)$$

165 and the coupling force vector applied over each substructure is defined by:

$$\mathbf{g}^N = \begin{Bmatrix} \mathbf{g}_i^N \\ \mathbf{g}_b^N \end{Bmatrix}, \quad \mathbf{g}^E = \begin{Bmatrix} \mathbf{g}_i^E \\ \mathbf{g}_b^E \end{Bmatrix} \quad (5)$$

166 The main assumption in this formulation is that the substructures are only coupled through
 167 the boundary Γ_b . Therefore, the coupling forces at interior DOFs for each substructure should
 168 be equal to zero:

$$\mathbf{g}_i^N = \mathbf{0}_i^N, \quad \mathbf{g}_i^E = \mathbf{0}_i^E \quad (6)$$

169 To solve this coupled problem, both displacement compatibility and force equilibrium con-
 170 ditions must be satisfied:

$$(Displacement compatibility): \quad \mathbf{x}_b^N = \mathbf{x}_b^E \quad (7)$$

$$(Force equilibrium): \quad \mathbf{g}_b^N + \mathbf{g}_b^E = \mathbf{0}_b \quad (8)$$

171 Therefore, by substituting (8) and (5) into (3), the following “coupled” numerical substruc-
 172 ture EOM is obtained:

$$\mathbf{M}^N \ddot{\mathbf{x}}^N + \mathbf{C}^N \dot{\mathbf{x}}^N + \mathbf{R}^N = \mathbf{p}^N + \begin{Bmatrix} \mathbf{0}_i^N \\ -\mathbf{g}_b^E \end{Bmatrix} \quad (9)$$

173 where \mathbf{g}_b^E is the coupling force vector from the experimental component, which includes all the
 174 effects associated with nonlinear restoring forces, nonlinear damping, and inertial forces, along
 175 with any external excitation that can be induced directly to the experimental substructure. In
 176 slow speed experiments, rate-dependent damping and inertial forces are ignored. The result is:

$$\mathbf{g}^E = \begin{Bmatrix} \mathbf{0}_i^E \\ \mathbf{g}_b^E \end{Bmatrix} = \mathbf{M}^E \ddot{\mathbf{x}}^E + \mathbf{C}^E \dot{\mathbf{x}}^E + \mathbf{R}^E - \mathbf{p}^E \quad (10)$$

177 while noting that the coupling vector \mathbf{g}_b^E is a function of displacement vector \mathbf{x}_b^N to satisfy (7):

$$\mathbf{x}^E = \begin{Bmatrix} \mathbf{x}_i^E \\ \mathbf{x}_b^E = \mathbf{x}_b^N \end{Bmatrix} \quad (11)$$

178 To obtain an admissible solution, compatibility and equilibrium must be satisfied for all
 179 boundary DOFs at all times. Therefore, an algorithm should be considered to prescribe dis-
 180 placements and/or forces at the boundary Γ_b for the solution of the dynamical system. Three
 181 different classes of algorithms are found in the literature:

182 **Displacement-based** After solving the EOM (9) of the numerical substructure Ω^N through
 183 a time-stepping integration algorithm, the output \mathbf{x}_b^N is commanded to the experimental
 184 substructure Ω^E for execution by actuator(s) to satisfy displacement compatibility at the
 185 boundary Γ_b . Displacement transducer(s) ensure that the command is achieved. Then,
 186 the coupling force \mathbf{g}_b^E is measured directly from the test specimen after displacement-
 187 controlled loading, using load cell sensors in a laboratory facility, and this measured output
 188 is inserted back into the numerical substructure Ω^N , to satisfy the equilibrium condition
 189 at the boundary Γ_b . This “hybrid loop” procedure is repeated until the simulation reaches
 190 the final simulation time.

191 **Force-based** Similar to displacement-based, the EOM of the numerical substructure Ω^N is
 192 solved, but now the coupling force \mathbf{g}_b^N is calculated and commanded to the experimental
 193 substructure Ω^E for execution by actuator(s). Load cell(s) ensure that the desired coupling
 194 force is achieved. Then, the displacement \mathbf{x}_b^E is measured directly from the test specimen

195 after force-controlled loading, and is fed back into the numerical substructure Ω^N , to
 196 satisfy displacement compatibility at the boundary condition Γ_b .

197 **Mixed-mode** Also called displacement-force control, this approach consists of calculating a
 198 set of displacements \mathbf{x}_b^N and coupling forces \mathbf{g}_b^N from the numerical substructure to be
 199 enforced on the experimental substructure simultaneously, satisfying compatibility and
 200 equilibrium over the boundary Γ_b .

201 In the context of hybrid simulation, a structural component of interest is usually selected
 202 from the reference structure to become the experimental substructure (i.e., physical specimen),
 203 as illustrated in Fig. 3. The choice for the experimental substructure can vary based on
 204 the research problem under consideration. But generally, the experimental substructure is
 205 comprised of elements with large uncertainty, or are expected to show a nonlinear response, for
 206 which appropriate models are not available, or for designs and materials that are perhaps new
 207 technologies and require further study.

208 As an illustrative example, consider a typical n -story shear building subjected to arbitrary
 209 excitation in the form of external forces $\mathbf{F}(t)$, and ground excitation $\ddot{x}_g(t)$. This reference
 210 structure may have any number of DOFs for added complexity and realism, but for the sake
 211 of establishing the abstract concepts for substructuring of an EOM, only the lateral DOFs are
 212 shown. In this case, the total load vector $\mathbf{p}(t)$ is defined as:

$$\mathbf{p}(t) = -\mathbf{M}\iota\ddot{x}_g(t) + \mathbf{F}(t) \quad (12)$$

213 where $\iota \in R^n$ is an inertial influence vector.

214 Here, the numerical substructure is assumed to behave elastically for simplicity, with a
 215 stiffness matrix \mathbf{K}^N , and restoring force $\mathbf{R}^N(\mathbf{x}^N) = \mathbf{K}^N\mathbf{x}^N$. The boundary point between the
 216 numerical and experimental substructure is indicated at the locations of the mass m_1 . Following
 217 a displacement-based algorithm, the boundary condition between the numerical and experimen-
 218 tal substructures is indicated with the DOFs $x_1^N(t)$ and $x_1^E(t)$, respectively. In an ideal world,
 219 the boundary condition calculated through integration of the numerical substructure would be
 220 perfectly executed via actuators located at the boundary with the experimental substructure
 221 with $x_1^N(t) = x_1^E(t)$ (displacement compatibility). Actuation of the physical specimen in the
 222 experimental substructure results in the generation of forces, measured by load cells. These
 223 coupling forces are returned to the numerical substructure as feedback forces, as illustrated in

224 Figure 3.

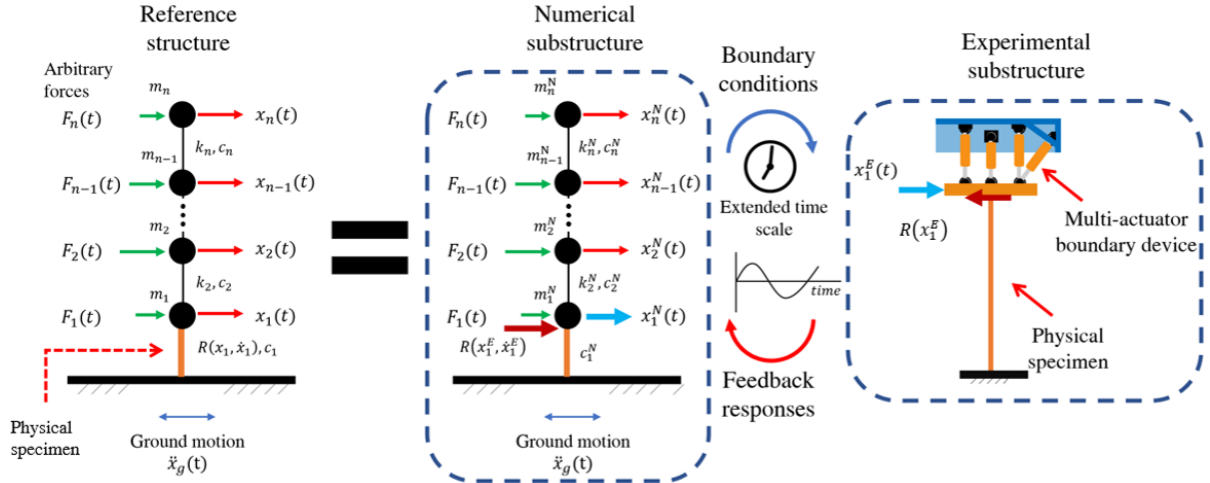


Figure 3: Conventional (slow-speed) hybrid simulation

225 In conventional (i.e., slow speed) hybrid simulation (HS) applications, the boundary conditions are imposed on the physical specimen over an extended time scale. As a result, velocity-
 226 and acceleration-dependent forces (i.e., damping and inertia) of the physical specimen are not
 227 acquired experimentally and must instead be modeled numerically. The feedback forces mea-
 228 sured in conventional HS, $R(x_1^E)$, are therefore only comprised of experimental restoring forces.
 229 Meanwhile, in RTHS applications, dynamic effects are included because the boundary condi-
 230 tions are imposed on the physical specimen at the real time according to the input excitation.
 231 Therefore, specimen inertial and damping forces are automatically incorporated into the feed-
 232 back forces. The inertial component of the experimental specimen must be removed from the
 233 numerical structure, as shown in Fig. 4.

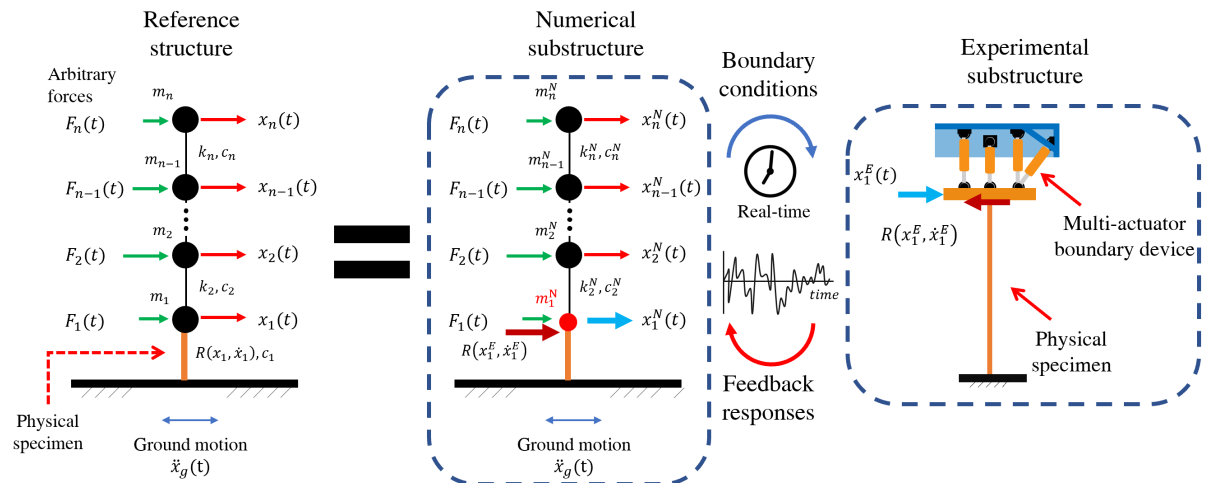


Figure 4: Real-time hybrid simulation

235 It is worth mentioning that other substructuring techniques have been used for hybrid
236 simulation testing, such as overlapping methods [28], where the substructures are overlapping
237 by more than the boundary nodes and can also share redundant elements. This overlapping
238 technique is conceived for the main purpose of alleviating the requirements on the number of
239 actuators at the boundary of experimental subassemblies. Similarly, [29] developed a weakly-
240 coupled HS where two DOFs of the physical specimen are measured experimental and one
241 DOF is obtained numerically. Also, switch control [30, 31] has been developed to command
242 forces in addition to displacements over the experimental substructure. The UT-SIM [32] is a
243 generalized distributed data exchange and communication protocol framework that integrates
244 numerous numerical analysis software and experimental testing equipment.

245 Certain multi-actuator devices have been developed for properly imposing the boundary
246 conditions to perform more complex hybrid simulations. These devices can be classified as (i)
247 multi-axial boundary devices, and (ii) individually attached actuators to a common physical
248 specimen, as illustrated in Fig. 5. In nearly all actuator setups, actuator dynamics will affect
249 trajectory tracking and stability of the hybrid simulation. In addition, actuators linked through
250 a stiff continuum (e.g., test specimen and/or loading fixtures) tend to be mechanically coupled
251 with forces in one actuator resulting forces in all other actuators. Control algorithms are
252 typically required in multi-actuator HS to satisfy synchronization between substructures, and
253 in multi-actuator RTHS to stabilize and tackle the dynamics inherent to actuators, as well as the
254 mechanical coupling between the actuators [33]. Successful operation of multi-actuator devices
255 also requires a mathematical understanding of the geometry of the motions, also commonly
256 known as the *kinematics*. Kinematic transformation algorithms capture the mapping needed
257 between each actuator and a Cartesian frames of reference.

258 2.2 Tracking algorithms in multi-actuator hybrid simulation

259 Tracking algorithms are mathematical formulations that help an actuator execute a command
260 displacement in a stable and timely manner. Studies have indicated addition of delays to the
261 closed-loop system in experiments where stiffness is dominant [34, 35], and addition of leads
262 where inertial forces are dominant [36]. The dynamics of actuators are considerably different
263 between slow speed and real-time hybrid tests, and so are the tasks of compensating.

264 In (conventional) HS, actuator displacements are typically applied in a repeated pattern
265 of slow ramp loading and pausing. A target displacement is first calculated by the numerical

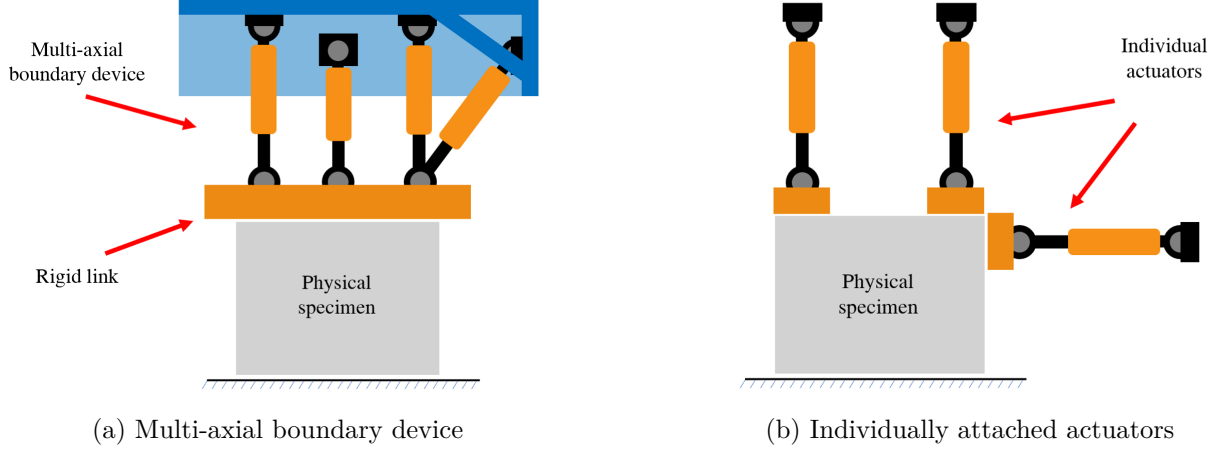


Figure 5: Multi-actuator configurations

266 substructure. Next, a controller generates a ramp-shaped command signal for the actuators to
 267 execute the target. The actuator is paused once the target trajectory is achieved and restoring
 268 forces are measured. This process is repeated for all other time steps [37, 38, 39, 40, 41].
 269 Ramp-hold algorithms may be insufficient however for compensating strong actuator coupling
 270 in multi-actuator platforms.

271 *Displacement- and force-control* are two types of commonly employed compensators in multi-
 272 actuator HS. Displacement-control is more appropriate for DOFs requiring a large actuator
 273 stroke and small specimen stiffness [42, 43, 44, 45]. DOFs with high stiffness (i.e., large force
 274 and small displacement variations) are best compensated with force-control [46]. *Mixed-control*
 275 is the combined use of both control methodologies. In mixed-control, the translations and
 276 rotations for lateral DOFs are compensated using displacement-control, and highly stiff axial
 277 DOFs are compensated using force-control [47, 30, 48, 49, 50, 51].

278 For an RTHS, response inaccuracies and instabilities will result, unless appropriate steps are
 279 taken toward compensating for the coupling between the actuators and dynamics of the multi-
 280 actuator device. The open-loop behavior of a servo-hydraulic actuator is inherently unstable.
 281 For the purpose of stabilization, the dynamics of a servo-hydraulic actuator is typically first
 282 stabilized using a proportional-integral-derivative (PID) compensator, known as an *inner-loop*
 283 [52]. Additional compensation techniques then take the form of outer-loops, which aim to
 284 achieve accurate target tracking. In the context of the RTHS example in Fig. 4, accurate
 285 tracking means $x_1^E(t) \rightarrow x_1^N(t)$ in a finite time, where $x_1^N(t)$ is the target boundary condition
 286 calculated from the numerical substructure, and $x_1^E(t)$ is the experimental realization (i.e.,
 287 measurements) of the boundary condition.

288 The majority of compensation algorithms used in RTHS today are based on displacement-
289 control. *Decoupled* and *coupled* control are the two types of real-time control used for multi-
290 actuator devices. Decoupled control refers to the case when individual actuators are treated as
291 single-input, single-output (SISO) systems, and are compensated for independently. Decoupled
292 controllers are easier to design, optimize, and have been widely used throughout the literature
293 [53, 54, 55, 56, 57, 58, 59, 60]. Such controllers may have limitations in experiments where the
294 coupling between the actuators is large, possibly due to presence of a very stiff physical spec-
295 imen. Coupled controllers treat actuators as multi-input, multi-output (MIMO) systems, and
296 compensate for the system-wide actuator dynamics [61, 62, 63]. These controllers are challeng-
297 ing to optimize for ideal stability and tracking behavior, due to the large number of parameters
298 that require tuning. Other forms of RTHS compensation are summarized as: mixed-control
299 [17], and acceleration-control [64, 65, 66]. The stiffness of the physical continuum that con-
300 nects the actuators largely determines the extent of the mechanical coupling in multi-actuator
301 devices. The literature listed have tackled application-specific coupling challenges. However, a
302 generalizable solution for realistic RTHS performance and stability does not exist to-date. [67]
303 developed a predictive indicator focused on assessing the stability of MDOF RTHS to use as a
304 design tool. [68] provided a sufficient condition for stability of RTHS with multiple actuators,
305 by employing the small gain theorem [69]. [70] found that analytical stability indicators are
306 not accurate for discrete systems. [71] investigates the critical time delay in multi-DOF RTHS
307 systems using the root locus technique. Usefulness of analysis models for predicting stability
308 and performance in experimental RTHS are highlighted.

309 2.3 Kinematics of multi-actuator loading assemblies

310 Kinematics refers to the mathematical operations that describe the geometry of motion and
311 forces in robotic assemblies with respect to time. The kinematic transformation of multi-
312 actuator systems must be well-understood for successful use of these devices in hybrid simula-
313 tion. There are two types of kinematic transforms: *Forward* and *Inverse*. Forward kinematic
314 transform considers the strokes in each individual actuator and sensing device (e.g., displace-
315 ment transducer) for deriving the position and orientation of the Cartesian boundary conditions
316 and forces. Inverse kinematic transformation uses the available information about the desired
317 positions of the boundary conditions to calculate what the strokes of individual actuators must
318 be.

319 Kinematic relationships are mathematically expressible via nonlinear equations. Solutions to
 320 the kinematic equations can be approximated for a finite range of motion, solved iteratively, or
 321 solved directly. [42] introduces a kinematic transformation matrix for performing a bi-directional
 322 HS. [43], [47], and [72] extend the prior development for handling of the geometric nonlinearities
 323 of a planer actuator setup. [44] presents two non-iterative kinematic transformation algorithms:
 324 linearized transformation for approximations, and nonlinear transformation which yield exact
 325 results. These approaches can be applied to real-time problems. [73] introduces an online
 326 iterative kinematic scheme for ensuring multi-actuator systems achieve a desired Cartesian
 327 motion. For real-time tests, iterative solutions however are not applicable. [63] and [60] present
 328 real-time kinematic transform methods based on direct and linearized approximations of the
 329 kinematic equations of motion.

330 A brief mathematical summary of kinematic transformations are provided next for the con-
 331 venience of the reader. A typical multi-actuator boundary device is comprised of several servo-
 332 hydraulic prismatic actuators moving a single highly stiff platform. These devices are known as
 333 *parallel manipulators*, and possess large load-carrying capacities due to the load sharing ability
 334 of the actuators. This quality is attractive in structural testing applications due to the large
 335 forces desired. A schematic of a generalized parallel manipulator is presented in Fig. 6.

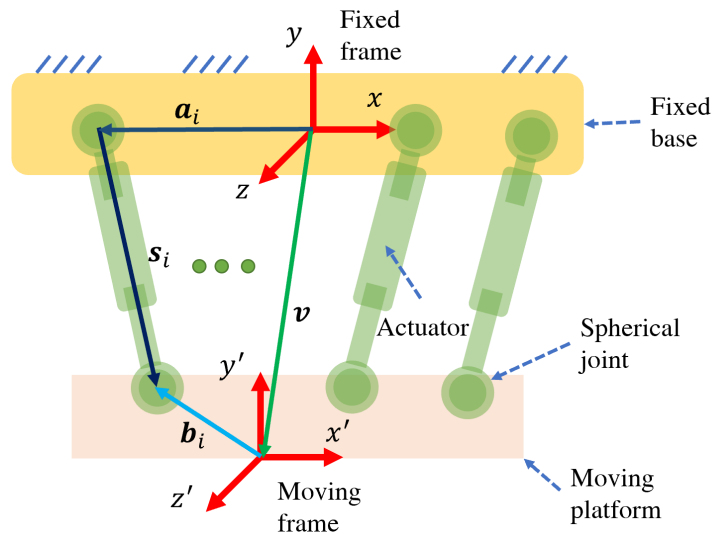


Figure 6: n-DOF parallel manipulator

336 A kinematic analysis of a parallel manipulator requires evaluation of the actuator environ-
 337 ment as a vector space. A Cartesian fixed frame of reference is typically selected in an arbitrary
 338 position, and a moving frame of reference is selected on the moving platform. In many ex-
 339 periments, the location of choice for the moving frame can be the centroid of the attachment

340 with the physical specimen. The linear strokes of the prismatic limbs (e.g., actuators) result in
 341 displacements and rotations of the moving platform.

342 With the frames of reference and parallel manipulator components visualized, the focus
 343 will next shift to kinematic transforms. Following the simulation of numerical substructures, to
 344 obtain the target Cartesian motion, an inverse kinematic transform calculates the stroke of each
 345 actuator. The vectors \mathbf{a}_i , \mathbf{b}_i , \mathbf{s}_i and $\mathbf{v} \in \mathbb{R}^3$, describe the position of the fixed and moving frames
 346 of reference, vector stroke of the actuators, and total translational vector, respectively. [52]
 347 introduces a sensitivity-based calibration method for multi-actuator devices based on external
 348 measurements. Incorporating a rotational matrix $\mathbf{A} \in \mathbb{R}^{3 \times 3}$, the three-dimensional forward
 349 kinematics of the actuated assemblies are:

$$\mathbf{s}_i = \mathbf{v} + \mathbf{A}\mathbf{b}_i - \mathbf{a}_i \quad (13)$$

350

$$|\mathbf{s}_i| = f(\boldsymbol{\omega}) \quad (14)$$

351 where $|\mathbf{s}_i|$ is the absolute length of actuator i for some target Cartesian motion of a moving
 352 frame of reference $\boldsymbol{\omega} = (x, y, z, \theta_x, \theta_y, \theta_z)^T$. The above derivations are based on an assumption
 353 that the load transfer elements (e.g., fixed and moving platforms) are rigid.

354 Actuator and sensor coordinate measurements are converted to Cartesian coordinates via the
 355 forward kinematic transform. In parallel manipulators, the forward transform is a challenging
 356 task that involves solving several implicit nonlinear equations per Eq. 15. Solutions to these
 357 equations can be achieved iteratively for HS or approximated using Taylor expansion around
 358 an stationary operation point for RTHS.

$$\boldsymbol{\omega} = f^{-1}(|\mathbf{s}|) \quad (15)$$

359 Regardless, compliance and slippage of multi-actuator connectors can induce wrong esti-
 360 mates of true Cartesian coordinates of the moving platform. Thus, some studies have proposed
 361 solutions to forward kinematics including these undesired effects. [74] proposed an online correc-
 362 tion method that adjusts Cartesian displacement commands by minimizing Cartesian displace-
 363 ment errors through optimization methods. [75] proposes a model-based adaptive kinematic
 364 method where the elastic deformations of connectors are included in a system model which is
 365 employed to compensate for estimation errors of Cartesian coordinates from actuator coordinate

366 measurements.

367 Finally, the kinematic transformation procedures described herein are generalizable for
368 multi-actuator setups with individually attached actuators per Fig. 5(b).

369 **3 Structural testing with multi-actuator devices**

370 This section explores many of the multi-actuator devices around the world dedicated to struc-
371 tural testing and hybrid simulation. There are three main reasons to consider the use of a
372 multi-actuator layouts in structural testing: (i) to increase loading capacity over a stiff and
373 high capacity physical specimen, (ii) to apply realistic 3D loading over specimens with multi-
374 axial boundary conditions, and (iii) for applications involving loading at multiple boundary
375 devices. Some of the commonly used multi-actuator devices include shake tables, boundary
376 condition devices, and shell element testers. The objective here is to introduce the available
377 capabilities and functionalities of these testing systems to the reader.

378 **3.1 Shake tables**

379 Shake tables are a class of actuated assemblies, where a moving platform is used to excite an
380 onboard structure. These devices are used to acquire the global nonlinear dynamical behaviors
381 of complete structures. Many large shake tables have been built around the world to test large and
382 full-scale structures. The *E-Defense* (6-DOF full-scale earthquake testing facility) is the world's
383 largest shake table, with a dimension of 20 m \times 15 m, a payload capacity of 12 MN, horizontal
384 motion of 1 m at > 9 m/s², and vertical motion of 0.5 m at > 15 m/s² [76, 77]. Tianjin
385 University is currently constructing an even larger shake table with underwater capabilities
386 [78]. The NHERI@UCSD shake table, shown in Fig. 7(a) has a 7.6 m \times 12.2 m platform, a
387 payload capacity of 20 MN [79], and was recently upgraded with additional actuators and servo-
388 hydraulics to have 6-DOF capabilities, with X-direction motion of 0.89 m at 5.9 g, Y-direction
389 motion of 0.38 m at 4.6 g, and Z-direction (vertical) motion of 0.127 m at 4.7 g [80]. In other
390 shake table facilities, size has been traded for flexible physically distributed testing capabilities.
391 Shake table arrays like those at the University of Nevada – Reno, and Tongji University, can
392 test long-span structures with multiple independent base excitations [81, 82]. Underwater shake
393 tables tests allow for experimentally attained hydrodynamic pressures for studying structural
394 behavior under seismic maritime environments [83, 84, 85]. Examples of shake table use in HS

395 and RTHS are provided in Sections 4.2 and 5.1.

396 3.2 Boundary condition devices

397 *Boundary condition devices* are mechanical manipulators made from several prismatic servo-
398 hydraulic actuators connected by swivel joints. The number of servo-hydraulic actuators is
399 typically equal to or higher than the number of DOFs expected from the boundary condition
400 device [47]. For instance, a 6-DOF boundary condition device has six actuators or more. Actua-
401 tors are pinned to a fixed base at one end, and a (stiff) moving platform at the other end. The
402 fixed base is typically attached to a rigid reaction wall, and the moving platform is attached to
403 the experimental substructure. Multi-axial boundary condition devices overcome the payload
404 limitations in shake tables and are advantageous in their flexibility for testing structures with
405 various configurations and experimental costs.

406 The Load and Boundary Condition Boxes (LBCBs) at the University of Illinois at Urbana-
407 Champaign are 6-DOF devices with force and position control capabilities, and X-direction
408 stroke and force capacities of 0.254 m and 2,402 kN, respectively. These capacities are 0.127
409 m and 1,201 kN in the Y-direction, and 0.127m and 3,603 kN in the Z-direction. The LBCBs,
410 shown in Fig. 7(b), are attached to highly stiff strong-wall and strong-floor reaction frames,
411 which allow flexibility in testing configurations [86]. Similar LBCB devices are also available in
412 smaller scales at the University of Illinois, the University of Southern California [87], and the
413 Institute of Engineering Mechanics, China Earthquake Administration in Beijing.

414 The Multi-Axial Subassemblage Testing (MAST) system is another type of boundary con-
415 dition device, first built at the University of Minnesota. The MAST is comprised of a highly
416 stiff moving platform (i.e., crosshead) that imposes boundary conditions and forces to the top
417 of the experimental substructure. The MAST has horizontal stroke and load capacities of 0.4 m
418 and 3,910 kN, and vertical capacity of 0.25 m and 5,870 kN, respectively [88]. Two new MAST
419 facilities were built recently at the Swinburne University of Technology and at the ETH Zürich
420 [89, 90].

421 The multi-use structural testing (HNU-MUST) system at MOE Key Laboratory of Building
422 Safety and Energy Efficiency at the Hunan University (HNU) is similar in design to the MAST,
423 with two horizontal and four vertical actuators with loading capacities of 4,000 kN and 20,000
424 kN, respectively. The stroke capabilities are 0.35m in the horizontal direction and 0.5 m in the
425 vertical direction [91]. The multi-directional hybrid testing system at the Structural Engineering

426 Laboratory of Polytechnique Montreal is a similar design to the MAST and has four horizontal
427 and four vertical actuators [92]. The Taiwan National Centre for Research on Earthquake
428 Engineering (NCREE) multi-axial testing system (MATS) is a self-reacting loading frame with
429 more than 15 actuators, which combine to enable 6-DOF boundary condition operation. MATS
430 was designed such that experimental substructure would be fixed from the top and excited from
431 the base [93].

432 **3.3 Shell element testers**

433 *Shell element testers* are experimental assemblies, composed of a large number of actuators,
434 that impose load combinations on four sides of shell elements. These devices are largely used
435 for testing of reinforced concrete (RC) shell elements and have led to important breakthroughs
436 in the field of mechanics of RC, including Compression Field Theory [94]. At the University of
437 Toronto, the Shear Panel Tester was developed in 1979 for in-plane tests, and the Shell Element
438 Tester was developed in 1984 for in-plane and out-of-plane tests and was upgraded to have 60
439 servo-hydraulic actuators. The UT10 Simulator is an augmentation to the Shell Element Tester
440 that allows hybrid testing of up to 10 elements simultaneously [95, 96]. Other shell element
441 testers are the Universal Element Tester at the University of Houston with 60 actuators [97],
442 and the Large Universal Shell Element Tester (LUSET) at the ETH Zürich with 100 actuators
443 illustrated in Fig. 7(c) [98]. HS and RTHS have not been implemented using shell element
444 testers to-date.

445 **3.4 Individually attached actuators**

446 As discussed in Section 2.1, individual actuators can be combined to realize a customized multi-
447 actuator boundary condition. Testing of frame structures with translational DOFs for instance
448 requires individually attached actuators to each story. The damped braced frame setup at the
449 Lehigh University real-time multi-directional (RTMD) large-scale testing facility, illustrated in
450 Fig. 7(d), is an example. In the testbed shown here, two stiff braced frames are attached to the
451 faces of the test frame to prevent out-of-plane motions [59, 99]. In other developments, actuators
452 were used for simulating both translational and rotational behaviors in the frame structures
453 [100, 53, 54, 101]. Many applications using individually attached actuators are discussed in
454 sections 5.1 and 6.1.



(a) Shake table, NHERI@UCSD



(b) LBCB, UIUC



(c) LUSET, ETH Zurich



(d) Damped Braced Frame, Lehigh RTMD

Figure 7: Types of multi-actuator devices

455 4 Multi-axial hybrid simulation (maHS)

456 The widespread use of (conventional) HS since the 1980s can be attributed to major advances
 457 in control and measurement techniques, substructuring formulations, test-pausing ability, and
 458 reliability in reproducing dynamic behaviors. This section provides a chronological summary of
 459 various illustrative maHS applications with LBCBs, MASTs, and other multi-actuator setups.

460 4.1 Multi-actuator applications

461 From the earliest days, developments in multi-actuator HS were driven by the need to simulate
 462 realistic seismic performances of structures in laboratory environments. The first multi-actuator

463 SSHS studies were on multi-story frame structures subject to uni-axial ground motions, where
464 actuators were attached to the each story to simulate floor translations [102, 103, 104]. Frame
465 structures with 6 and 8 actuator configurations were studied in [105] and [106], respectively.
466 [107] presents a a bi-directional two-actuator test setup for evaluating a bi-axial ground motion
467 on a frame.

468 4.2 Multi-axial applications

469 Only planer hybrid simulation were considered up until the mid-1990s, as the dynamics of
470 planar structures are more easily verifiable on a shake table. The limitations of the planar
471 frameworks are that multi-component excitations and 3D strength envelopes of structures are
472 not incorporated into the hybrid test. Extensions of the HS method into the multi-axial setting
473 requires tackling of the geometric nonlinearities resulting from the actuator kinematics, and
474 compensation for the mechanical coupling introduced when a stiff physical specimen is shared
475 among multiple actuators. The work in the multi-axial domain began with planar (i.e., 3-DOF)
476 developments [42, 43, 72, 100, 44].

477 In the early 2000s, great emphasis was placed on earthquake engineering and hybrid simula-
478 tion research through the Network for Earthquake Engineering Simulation (NEES) program [22].
479 The MUST-SIM facility at the University of Illinois was influential in advancing multi-axial HS
480 methods to enable research. [86] outlines the use of full-scale and 1/5th-scale LBCBs at MUST-
481 SIM for vertical accelerations assessment on shear capacity and demand of RC bridge piers in a
482 geographically distributed HS between University of Illinois at Urbana-Champaign and Lehigh
483 University. [108] presents a mixed-mode control strategy for HS of a skewed RC bridge. [109]
484 concludes from a vulnerability study of RC bridge piers that without consideration of vertical
485 accelerations, the severity of earthquake-induced damages can be widely underestimated. [110]
486 conducts a multi-axial test on RC slender walls using two LBCBs connected over a rigid link,
487 to achieve the necessary vertical loads and overturning moments. Multiple LBCBs were used in
488 a four-span bridge test, where the piers were physical and the deck was numerically evaluated
489 [111, 112]. The results from this study were compared to analytical simulations for verification.
490 [45] studies moment frames where two LBCBs test a full-scale beam-column connection, while
491 the rest of the assembly is modeled numerically. [113] performs multi-axial simulation on an
492 RC frame structure under pulse-type ground motion and evaluates shear failures in pre-1970
493 structures. Despite immediate failure of the columns, the 10-story building structure did not

494 under go collapse.

495 The MAST facilities at the University of Minnesota and the Swinburne University of Sci-
496 ence and Technology enable a broad scope of SSHS experiments. [88] and [114] discuss the
497 possibilities for hybrid simulation using the MAST systems. [115] uses the MAST system to
498 generate collapse fragility curves of an RC column using quasi-static testing and SSHS. The
499 probability of collapse is discovered to be less when column is SSHS tested and the realistic
500 boundary conditions are imposed. Building on this research, [116] also evaluates the effective-
501 ness of carbon fiber reinforcement polymer repairs in restoring earthquake-damaged columns to
502 their original performances. [117] implements a 6-DOF seismic hybrid simulation of RC bridge
503 piers including excitation in the vertical direction.

504 A vast body of literature is designated to multi-axial and multi-actuator HS frameworks.
505 Because of the iterative algorithms embedded in these frameworks, they are, however, unable
506 to produce real-time results. The next section will explore the various developments in RTHS.

507 5 Multi-axial real-time hybrid simulation (maRTHS)

508 Although RTHS and SSHS are similar in architecture, successful implementation of each method
509 requires solving different challenges. Sensors, computers, and actuators used in real-time tests
510 must acquire, process, and execute at higher speeds. A complete RTHS loop: numerical integra-
511 tion, kinematic transformation, actuator compensation, physical execution, and measurement
512 of feedback forces, must be completed in a very small time increment. In addition, the fast
513 loading speeds required to perform RTHS create frequency-dependent actuator dynamics and
514 often reveal nonlinearities. Fast operation also impacts the interactions between an actuator
515 setup and the physical structure, in what is known as *control-structure interaction* [33]. This
516 section presents literature in RTHS and is divided in two subsections on multi-actuator and
517 multi-axial testing, respectively.

518 5.1 Multi-actuator applications

519 The earliest multi-actuator RTHS targeted a simple portal frame [53, 54], where a column with
520 a 2-DOF boundary condition at the top is experimentally substructured. Two-actuator setup
521 is connected to a highly stiff loading bracket, which deforms the experimental column through
522 translation and rotation. The oscillating instabilities that resulted from actuator coupling were

523 solved using a delay compensation algorithm.

524 The next set of multi-actuator RTHS experiments focused on dynamic substructuring of
525 mass-dashpot-spring (MDS) systems arranged in a series configuration. [55] explores a triple
526 MDS system, while [56] studies two systems of four and five MDSs, respectively. The boundary
527 condition between the substructures are realized by connecting actuators to the experimental
528 springs on either side of the middle mass. MDS systems allow for dynamic coupling studies by
529 varying the stiffness of the spring elements. These systems are typically limited to only two
530 actuators.

531 Shake tables are useful for testing of multi-story structures, and have been used in RTHS
532 studies. [118] introduces a shake table RTHS for a two-story structure, with an experimental
533 first story, and a numerical second story. A shake table and an actuator excite the base and
534 mass of the first story, respectively. [119] studied a three-story structure where the second story
535 was experimentally tested. Applied accelerations for the base and mass are first converted to
536 displacement commands. [120] reviews various RTHS tests with shake tables. Most of the
537 tests discussed are however limited to 1-DOF actuation. [121] studied full-scale rolling bearings
538 used as floor isolation systems using multi-axial RTHS shake table tests in the Natural Hazards
539 Engineering Research Infrastructure (NHERI) Experimental Facility at Lehigh University.

540 Several RTHS studies are dedicated to multi-story frame structures. [61] conducts a nu-
541 merical RTHS of a three-story steel frame structure with a magnetorheological (MR) damper
542 installed at the first story. The author proposes a coupled model-based controller for the three-
543 actuators exciting the frame in simulation. [62] evaluates a two-story steel moment resisting
544 frame (MRF) with a first-story MR damper in three different RTHS configurations: fully nu-
545 merical, experimental MR damper with a numerical frame, and fully experimental frame with
546 numerical mass. [59], [99], and [122] explore the passive and semi-active use of MR dampers for
547 vibration mitigation in a three-story MRF. Three actuators excite a damped brace frame con-
548 taining three MR dampers as part of the experimental substructure, and the MRF is modeled
549 numerically. [123] studies the behavior of a two-story steel frame structure with an experimen-
550 tal first story column. A setup of three actuators (i.e., two vertical and one lateral) drive the
551 boundary conditions for the column. A nonlinear finite element analysis program for hybrid
552 testing is also discussed which shortens the computational time.

553 **5.2 Multi-axial applications**

554 Multi-axial RTHS is challenging due to the need for fast experimental hardware, high levels
 555 of actuator coupling, and accuracy of the kinematic calculations. The boundary condition
 556 devices used for multi-axial RTHS require different algorithms for kinematic transformations
 557 and actuator compensations than those listed in section 4. Iterative solutions developed for slow
 558 speed testing must be replaced with rapid solutions, to generate stable and accurate trajectories
 559 in one or few discrete time steps.

560 Two classes multi-axial real-time hybrid simulation (maRTHS) frameworks have been pro-
 561 posed in the recent years for boundary condition devices such as the LBCB and the MAST.
 562 The difference between these approaches is in how actuator compensation is conducted. [63]
 563 proposes a coupled compensation, while [60] and [124] propose a decoupled compensation.

564 The general architecture of both frameworks involves directing target displacements and
 565 rotations obtained from the numerical substructure through an outer-loop controller, to compute
 566 control signals for boundary condition device execution. Model-based outer-loop controllers
 567 are proposed in these frameworks, for addressing the dynamic coupling that exists between
 568 the actuators in the boundary condition devices. Individual hydraulic actuators are identified
 569 with a transfer function model $G_i(s)$, where i is the actuator index. Next, the kinematic
 570 relationships for the boundary condition devices are acquired, including Jacobian matrices from
 571 the linearization of Eq.(15). In [63], the Jacobian and the diagonal transfer function matrix
 572 of the actuators are combined to create a MIMO transfer system representing the nominal
 573 boundary condition device dynamics in Cartesian coordinates:

$$\hat{\mathbf{G}}(s) = \begin{bmatrix} \hat{G}_{11}(s) & \hat{G}_{12}(s) & \dots \\ \vdots & \ddots & \\ \hat{G}_{n1}(s) & & \hat{G}_{nn}(s) \end{bmatrix} = \mathbf{J}^{-1} \begin{bmatrix} G_1(s) & & \\ & \ddots & \\ & & G_n(s) \end{bmatrix} \mathbf{J} \quad (16)$$

574 where n is the total number of hydraulic actuators used in the boundary condition device. Next,
 575 feedforward and feedback controllers are designed as coupled systems according to the model-
 576 based architecture proposed in [61]. Lastly, feedback forces from the experiment coordinate
 577 transformed and returned to the controller responsible for carrying out the computation for the
 578 next time step, thus closing the maRTHS loop.

579 Studies on the rotational DOFs were found to cause oscillating instabilities, due to the lack
 580 of sufficient control authority provided by the coupled controller in this study. Tuning and

581 optimization are a challenging task, due to the numerous parameters in these compensators.

582 To minimize the role that dynamic coupling plays in the compensation task, [60] proposed
583 an maRTHS framework with the compensation taking place in the actuator frame of reference
584 as opposed to Cartesian coordinates where coupling is substantial. Cartesian signals (e.g.,
585 target and measured) are first converted to actuator signals via kinematic transformation. SISO
586 controllers are designed for each individual actuator following the system identification and
587 acquisition of the diagonal transfer matrix $\mathbf{G}(s)$. The decoupled maRTHS framework has also
588 been extended for studies where use of more than one boundary condition device is desired
589 [124].

590 5.3 Multi-axial real-time testing in other engineering disciplines

591 Due to the listed challenges, applications of maRTHS are rare and few in the field of Civil Engi-
592 neering. Methodologies similar to RTHS have been implemented in other engineering disciplines
593 and are commonly referred to as *Hardware-in-the-loop* (HIL) tests. The HIL uses of serial and
594 parallel robotics common in Aerospace and Mechanical applications involving aircraft, automo-
595 biles, and spacecrafts. The first uses of multi-axial robots for vibration based applications were
596 by V. E. Gough for tire testing, K. L. Cappel and D. Stewart for flight simulators [125, 126].
597 These replicas of aircraft cockpits installed on parallel manipulators are simulating the flight
598 environment for pilot training and other in-flight studies. In the automotive industry HIL is
599 used for rapid prototyping. HIL constitutes a synergy between various physical components
600 (e.g., powertrain, axles, and chassis) and virtual models (e.g., environment conditions, driver
601 commands, and road profile) [127, 128]. [129] and [130] introduced an HIL test rig for mecha-
602 tronic vehicle axles. A hexapod manipulator with six hydraulic actuators imposes multi-axial
603 forces and torques. In the space industry, spacecrafts are often multi-axial vibration tested for
604 system identification, verification of mathematical models, and simulation of in-flight shocks
605 and vibrations. The Mechanical Vibrations Facility (MVF) at the Glenn Research Center con-
606 tains a vibration table with 16 vertical and 4 horizontal actuators, used for modal testing [131].
607 Other commercial products, such as the MTS Multi-axial Simulation Tables [132], have been
608 used for various multi-axial dynamic tests.

609 6 Current challenges and opportunities

610 Hybrid simulation with multiple actuators is an active topic of research and has proven to be an
611 effective tool for various investigations and applications. However, a great deal more research
612 is needed to establish generalizable theories and build the capacity needed to truly exploit
613 hybrid simulation, and especially RTHS, to study complex structural engineering problems.
614 This section sheds light on some of the remaining challenges and unanswered questions in this
615 domain. In doing so, the aim is to share research insights, and to direct the attention of the
616 research community to existing research gaps and future research directions.

617 6.1 Robustness of multi-actuator closed-loop systems

618 Design of an RTHS test determines the quality of the tracking behavior achieved at the boundary
619 conditions and the closed-loop robustness to uncertainty. When stability and performance
620 are critical in validation studies, emphasis is typically placed on compensation design, and
621 when easier compensation design is desired, emphasis is on the choice for the RTHS partition
622 [67]. For multi-actuator setups, the operational challenge is increased due to the dynamic
623 coupling that exists between actuators. Coupled compensation may be a more rational approach
624 for developing multivariate models. For instance, multivariate robust control approaches take
625 into account all the coupling effects as uncertainties. Decoupled compensation is easier to
626 program, and allows for adaptive control developments in actuator space. However, the effects
627 of stiff specimen on Cartesian performance need to be studied. Use of adaptive and robust
628 compensation methods should be explored for improving the robustness of RTHS experiments.

629 Most applications in the maRTHS domain have used displacement-based compensation al-
630 gorithms. Displacement compensation is not suitable for testing highly stiff physical specimen,
631 as the smallest actuator motion result in sharp increases in reaction forces from the physical
632 specimen [46]. Another challenge with testing a stiff physical specimen is in the accurate mea-
633 surement of small multi-DOF deformations. Force compensation allows for a more stable and
634 accurate control of highly stiff DOFs. Displacement compensation also does not allow for main-
635 taining a prescribed force level (e.g., gravity forces) over a physical specimen. Gravity forces
636 result in application of axial forces which can alter with the failure mode and capacity of phys-
637 ical specimen [133]. The MTS control software is a generic kinematic transformation tool that
638 provides a layer of force control loop is included for over constrained systems when the number

639 of actuators exceeds the number of controlled DOFs [134]. Therefore, incorporation of force and
640 displacement compensations into maRTHS can combine the benefits of both approaches and
641 improve the realism of this experimental framework.

642 A key aspect of hybrid simulation is the black-box and reference-free nature of the experi-
643 mental substructures. Quantifying the uncertainty associated with the experimental substruc-
644 turing, and exploiting this information for the design of a suitable controller and updating
645 of the numerical substructure are critical to the accuracy and confident generalization of this
646 method [135, 136]. [137] presents foundational ideas for uncertainty quantification via a modular
647 framework that divides RTHS into smaller units on multi-rate coordination, actuator control,
648 state estimation and model updating, stability and performance indicators, and real-time deci-
649 sion making. Multivariate representation of uncertainty for a multi-actuator system remains a
650 major challenge.

651 6.2 Mechanical design of multi-actuator loading assemblies

652 The choice for the closed-kinematic chain architecture of multi-actuator loading assemblies will
653 dictate the success of the kinematic planning. Consider the linearization of Eq.(15), which
654 generates a Jacobian matrix \mathbf{J} . Certain arrangements of the actuators over the test specimen
655 or loading platform may result in formulation of a singular \mathbf{J} matrix [138]. When designing
656 multi-actuator assemblies, the presence of singularities must be explored over a given trajectory
657 workspace. In addition, loading platform must be designed to have optimal coupling, stiff-
658 ness, and capacity. This challenge exists for individually attached non-modular multi-actuator
659 configurations too.

660 The next challenge is with multi-actuator hardware requirements. RTHS with multiple
661 actuators require large hydraulic capabilities (e.g., accumulators for flow demands, manifolds
662 with additional accumulators for fast transient response) [139]. For instance, [140] provide
663 details of the hydraulic power system for the NHERI@UCSD outdoor shake table, with a model
664 of the hydraulic accumulators.

665 Other mechanical design challenges include interactions among the various fixtures including
666 actuator friction, bearing slippage, moving platform inertia, and flexibility of the loading and
667 support assemblies. These phenomena create erroneous load cell and displacement transducer
668 measurements, which result in inaccurate simulations [92]. Therefore, the contribution of these
669 phenomena must be minimized through measurement and compensation. For example, [73]

670 provide an online positioning correction algorithm for multi-actuator loading platforms with
671 flexible fixtures (i.e., reaction wall and floor). Also, adaptive kinematic transformations were
672 proposed by [75] to compensate the errors associated to fixture compliance in multi-axial hybrid
673 simulation at slow speeds. Future developments should focus on strategies to circumvent fixture
674 properties on the accuracy of multi-axial real-time testing.

675 6.3 Time constraints and computational efforts

676 Real-time solutions to the numerical substructure, model updating, actuator compensation, and
677 coordinate transformation constitute most of the computational efforts in RTHS. With more
678 actuators and increased degree of actuator coupling, the computational efforts grow further.
679 Most computational platforms however cannot execute real-time simulations at the rapid rates
680 typically used in RTHS testing (e.g., 2048 Hz or higher). Parallel computing is an afford-
681 able way of overcoming computational constraints while meeting the increased computational
682 demands for real-time multi-actuator applications. [141] introduces a platform for parallel com-
683 puting of complex numerical substructures on standard off-the-shelf multi-core computers. Field
684 programmable gate arrays (FPGAs) are also affordable means to speed up the computational
685 capabilities [142].

686 Efficient computational programs (e.g., codes) for the numerical substructures are rarely
687 available. OpenSees finds it challenging to meet the efficiency requirements for real-time testing.
688 Instead, researchers often resort to the Bouc-Wen simulation code [143]. [144] developed an
689 efficient Timoshenko hysteretic beam model with nonlinear behavior. [145] developed a state-
690 space formulation for structural analysis with plastic and geometric nonlinearities.

691 6.4 Validation of multi-actuator RTHS

692 Another challenge with multi-actuator HS and RTHS applications is validation. In many appli-
693 cations, RTHS results are validated against numerical analysis results. This approach is however
694 difficult when the nonlinearity and physics of the experimental substructure are unknown. The
695 need for validation grows stronger as RTHS methods grow more complicated.

696 New benchmark problems are needed for advancing new technologies in maHS and maRTHS.
697 [146] presented an RTHS benchmark control problem which offered challenges of unmodeled
698 dynamics and uncertainty. A nonlinear RTHS benchmark control problem is currently in the
699 works.

700 **6.5 Other applications regarding multi-axial testing**

701 Other hybrid testing applications pertain to the multi-physics problems, which refers to si-
702 multaneous presence and coupling of physical phenomena in a single system or simulation.
703 Multi-physics problems involving fluid-solid interaction have been studied in recent years. Some
704 examples of hybrid simulation with wind-structure behavior as the focus of the study are: off-
705 shore monopile wind turbines [147], semi-submersible floating wind turbines [148], aeroelastic
706 base-pivoting building model [36], and wind-tunnel model for flexible bridges [149]. For multi-
707 physics seismic research, underwater shake tables are useful for realizing hydrodynamic pressures
708 [83, 84, 85]. Coupling of structural and thermal loads have also been explored [150, 151, 19].
709 Multi-physics cyber-physical testing to examine complex systems involving thermal and struc-
710 tural coupling is also being developed [152, 153]. Traditional multi-actuator approaches dis-
711 cussed in this review paper may not be suitable for multi-physics problems. Hence, new gener-
712 alizable approaches should be explored.

713 **7 Concluding remarks**

714 Multi-actuator hybrid simulation is the process of emulating the dynamical behavior of a struc-
715 tural system through closed-loop simulation of its constituent substructures (i.e., numerical and
716 experimental) via multiple actuators. This methodology serves as a middle ground between
717 pure numerical simulation, which offers rapidness, and full experimental testing, which offers
718 realism and means for validation. In addition, multi-actuator hybrid simulation offers flexibility
719 which addresses a broad range of experimental configurations.

720 This review paper highlights the historical roots, evolution and key enablers of HS and RTHS
721 methods. A greater emphasis has been placed on multi-actuator and multi-axial test setups,
722 as single-actuator HS and RTHS have already been discussed in other review literature. The
723 general framework for the methodology are outlined, starting with the concepts of substructur-
724 ing, compensation, and kinematic transformation, and the fundamental differences between HS
725 and RTHS are highlighted. Capabilities of several experimental facilities around the world are
726 presented and their significance to HS and RTHS are discussed. A thorough review of multi-
727 actuator and multi-axial HS and RTHS are next provided. Finally, several insights are provided
728 on current challenges and future research directions.

729 **Acknowledgements**

730 The author's gratefully acknowledges the *Research Coordination Network in Hybrid Simulation*
731 *for Multi-hazard Engineering*, supported by the National Science Foundation grant No. 1661621.

732 **References**

733 [1] M. S. Williams and A. Blakeborough. Laboratory testing of structures under dynamic
734 loads: An introductory review. *Philosophical Transactions of the Royal Society A: Mathe-*
735 *matical, Physical and Engineering Sciences*, 359(1786):1651–1669, 2001. ISSN 1364503X.
736 doi: 10.1098/rsta.2001.0860.

737 [2] Narutoshi Nakata, Shirley J. Dyke, Jian Zhang, Gilberto Mosqueda, Xiaoyun Shao,
738 Hussam Mahmoud, Monique H. Head, Michael Erwin Bletzinger, Genez A. Marshall,
739 Ge Ou, and Cheng Song. Hybrid simulation primer and dictionary, 2014. URL
740 https://mechs.designsafe-ci.org/media/cms_page_media/965/Primer.pdf.

741 [3] Motohiko Hakuno, Masatoshi Shidawara, and Tsukasa Hara. Dynamic destructive test of
742 a cantilever beam, controlled by an analog-computer. *Proceedings of the Japan Society*
743 *of Civil Engineers*, 1969(171):1–9, 1969. ISSN 1884-4936. doi: 10.2208/jscej1969.1969.
744 171{_}1. URL http://ci.nii.ac.jp/naid/130003978834/http://joi.jlc.jst.go.jp/JST.Journalarchive/jscej1969/1969.171_1?from=CrossRef.

745 [4] Koichi Takanashi, Kuniaki Udagawa, Matsutaro Seki, Tsuneo Okada, and Hisashi Tanaka.
746 Nonlinear Earthquake Response Analysis of Structures by a Computer-Actuator On-Line
747 System. *Bulletin of Earthquake Resistant Structure Research Center*, (8):1–17, 1975. doi:
748 10.3130/aijsaxx.229.0.

749 [5] Robert D Hanson and N Harris McClamroch. Pseudo dynamic test method for inelastic
750 building response. In *Proceedings of the 8th World Conference on Earthquake Engineering*,
751 pages 123–134, San Francisco, 1984.

752 [6] Stephen A Mahin and Pui-shum B Shing. Pseudodynamic method for seismic testing.
753 *Journal of Structural Engineering*, 111(7):1482–1503, 1985.

754 [7] Masayoshi Nakashima, Hiroto Kato, and Eiji Takaoka. Development of real-time pseudo
755 dynamic testing. *Earthquake Engineering and Structural Dynamics*, 21(1):79–92, 1992.

757 [8] Andrew Plummer. Electrohydraulic servovalves - past, present, and future. In *10th*
758 *International Fluid Power Conference*, pages 405–424, Dresden, 2016.

759 [9] R. H. Maskrey and W. J Thayer. A brief history of electrohydraulic servomecha-
760 nisms. *Journal of Dynamic Systems Measurement and Control*, 1978. URL http://www.mylesgroupcompanies.com/moog_pdfs/MoogBriefHistoryofServovalves.pdf.

762 [10] Hans Moravec. *Robot: Mere Machine to Transcendent Mind*. Oxford University Press,
763 2000. ISBN 0195136306.

764 [11] L. Javier Malvar and C. Allen Ross. Review of Strain Rate Effects for Concrete in Tension.
765 *ACI Materials Journal*, 95:735–739, 1998.

766 [12] Matthew P. Murray, Stephen P. Rowell, and Trace A. Thornton. Effects of High Strain
767 Rates on ASTM A992 and A572 Grade 50 Steel. Technical report, 2014.

768 [13] Yunbyeong Chae, Minseok Park, Chul-young Kim, and Young Suk. Experimental study
769 on the rate-dependency of reinforced concrete structures using slow and real-time hybrid
770 simulations. *Engineering Structures*, 132:648–658, 2017. ISSN 0141-0296. doi: 10.1016/j.j.
771 engstruct.2016.11.065. URL <http://dx.doi.org/10.1016/j.engstruct.2016.11.065>.

772 [14] W. Ghannoum, V. Saouma, G. Haussmann, K. Polkinghorne, M. Eck, and D.-H Kang.
773 Experimental Investigations of Loading Rate Effects in Reinforced Concrete Columns.
774 *Journal of Structural Engineering*, 138(8):1032–1041, 2012. doi: 10.1061/(ASCE)ST.
775 1943-541X.0000540.

776 [15] Min Li and Hongnan Li. Effects of Loading Rate on Reinforced Concrete Beams. In *17th*
777 *World Conference on Earthquake Engineering*, Lisbon, 2012.

778 [16] Guoxi Fan, Yupu Song, and Licheng Wang. Experimental study on the seismic behavior of
779 reinforced concrete beam-column joints under various strain rates. *Journal of Reinforced
780 Plastics & Composites*, 33(7):601–618, 2014. doi: 10.1177/0731684413512706.

781 [17] Narutoshi Nakata, Richard Erb, and Matthew Stehman. Mixed force and displacement
782 control for testing base-isolated bearings in real-time hybrid simulation. *Journal of Earth-
783 quake Engineering*, 23(6):1055–1071, 2019. doi: 10.1080/13632469.2017.1342296.

784 [18] Sarah Tell, Andreas Andersson, Amirali Najafi, Bill F. Spencer Jr., and Raid Karoumi.
785 Real-time hybrid testing for efficiency assessment of magnetorheological dampers to mit-
786 igate train-induced vibrations in bridges. *International Journal of Rail Transportation*, 0
787 (0):1–20, 2021. doi: 10.1080/23248378.2021.1954560.

788 [19] Xuguang Wang, Robin E. Kim, Oh-Sung Kwon, In-Hwan Yeo, and Jae-Kwon Ahn. Con-
789 tinuous real-time hybrid simulation method for structures subject to fire. *Journal of Struc-
790 tural Engineering*, 145(12):04019152, 2019. doi: 10.1061/(ASCE)ST.1943-541X.0002436.

791 [20] D de Klerk, D J Rixen, and S N Voormeeren. General Framework for Dynamic Sub-
792 structuring: History, Review and Classification of Techniques. *AIAA Journal*, 46(5):
793 1169–1181, 5 2008. ISSN 0001-1452. doi: 10.2514/1.33274. URL <https://arc.aiaa.org/doi/10.2514/1.33274>.

794

795 [21] Masayoshi Nakashima, J. McCormick, and T. Wang. Hybrid Simulation: A historical
796 perspective. In Victor Saouma and Mettupalayam Sivaselvan, editors, *Hybrid Simula-
797 tion: Theory, Implementation, and Applications*, chapter 1, page 3–12. Taylor & Francis,
798 2008. URL <https://books.google.com/books?hl=en&lr=&id=fJzmEkGuzWQC&oi=fnd&pg=PA3&ots=Q0essMEFmL&sig=lr3JCp9svu8NnDJiXK9ygUJgw2Q>.

799

800 [22] Daniel Gomez, Shirley J. Dyke, and Amin Maghreh. Enabling role of hybrid simulation
801 across NEES in advancing earthquake engineering. *Smart Structures and Systems*, 15(3):
802 913–929, 2015. ISSN 17381991. doi: 10.12989/sss.2015.15.3.913.

803

804 [23] D P McCrum and M S Williams. An overview of seismic hybrid testing of engineering
805 structures. *Engineering Structures*, 118:240–261, 2016. ISSN 01410296. doi: 10.1016/j.
806 engstruct.2016.03.039.

807

808 [24] Masayoshi Nakashima. Hybrid simulation: An early history. *Earthquake Engineering &
809 Structural Dynamics*, (March):1–14, 4 2020. ISSN 00988847. doi: 10.1002/eqe.3274. URL
810 <http://doi.wiley.com/10.1002/eqe.3274>.

811 [25] Stathis N Bousias. Seismic Hybrid Simulation of Stiff Structures: Overview and Current
812 Advances. *Journal of Structures*, 2014:1–8, 2014. ISSN 2356-766X. doi: 10.1155/2014/
813 825692. URL <http://www.hindawi.com/archive/2014/825692/>.

812 [26] Anil K Chopra. *Dynamics of Structures: Theory and Applications to Earthquake Engi-*
813 *neering*. Prentice Hall, fourth edi edition, 2012. ISBN 978-0-13-285803-8.

814 [27] Xu Huang and Oh-Sung Kwon. An integrated simulation method for coupled dynamic
815 systems. *Computer-Aided Civil and Infrastructure Engineering*, 35(10):1115–1131, 2020.
816 doi: <https://doi.org/10.1111/mice.12556>. URL <https://onlinelibrary.wiley.com/doi/abs/10.1111/mice.12556>.

817

818 [28] Javad Hashemi and Gilberto Mosqueda. Innovative substructuring technique for hybrid
819 simulation of multistory buildings through collapse. *Earthquake Engineering & Structural
820 Dynamics*, 43:2059–2074, 2014.

821 [29] Georgios Giotis, Oh-Sung Kwon, and Shamim A. Sheikh. Weakly coupled hybrid sim-
822 ulation method for structural testing: Theoretical framework and numerical verifica-
823 tion. *Journal of Structural Engineering*, 146(2):04019196, 2020. doi: 10.1061/(ASCE)
824 ST.1943-541X.0002492.

825 [30] Peng Pan, Masayoshi Nakashima, and Hiroshi Tomofuji. Online test using displacement-
826 force mixed control. *Earthquake Engineering and Structural Dynamics*, 34(8):869–888,
827 2005. ISSN 00988847. doi: 10.1002/eqe.457.

828 [31] T. Y. Yang, Dorian P. Tung, Yuanjie Li, Jian Yuan Lin, Kang Li, and Wei Guo. Theory
829 and implementation of switch-based hybrid simulation technology for earthquake engineer-
830 ing applications. *Earthquake Engineering and Structural Dynamics*, 46(14):2603–2617,
831 2017. ISSN 10969845. doi: 10.1002/eqe.2920.

832 [32] Xu Huang and Oh-Sung Kwon. A Generalized Numerical/Experimental Distributed
833 Simulation Framework. *Journal of Earthquake Engineering*, 24(4):682–703, 2020. doi:
834 10.1080/13632469.2018.1423585.

835 [33] S. J. Dyke, Billie F. Spencer, Jr., P. Quast, and M. K. Sain. Role of Control-Structure In-
836 teraction in Protective System Design. *Journal of Engineering Mechanics*, 121(2):322–338,
837 1995. ISSN 0733-9399. doi: 10.1061/(ASCE)0733-9399(1995)121:2(322). URL <http://ascelibrary.org/doi/10.1061/%28ASCE%290733-9399%281995%29121%3A2%28322%29>.

838

839 [34] Pui-shum B Shing and Stephen A Mahin. Cumulative experimental errors in pseudo-

840 dynamic tests. *Earthquake Engineering and Structural Dynamics*, 15(4):409–424, 1987.
841 ISSN 10969845. doi: 10.1002/eqe.4290150402.

842 [35] Pui-shum B. Shing and Stephen A. Mahin. Experimental Error Effects in Pseudodynamic
843 Testing. *Journal of Engineering Mechanics*, 116(4):805–821, 1990. ISSN 0733-9399. doi:
844 10.1061/(asce)0733-9399(1990)116:4(805).

845 [36] Moniruzzaman Moni, Youchan Hwang, Oh-Sung Kwon, Ho-Kyung Kim, and Un Yong
846 Jeong. Real-time aeroelastic hybrid simulation of a base-pivoting building model in a wind
847 tunnel. *Frontiers in Built Environment*, 6, 2020. ISSN 2297-3362. doi: 10.3389/fbuil.2020.
848 560672. URL <https://www.frontiersin.org/article/10.3389/fbuil.2020.560672>.

849 [37] Koichi Takanashi and K. Ohi. Earthquake response analysis of steel structures by rapid
850 computer-actuator on-line system. *Bulletin of Earthquake Engineering*, 16:103–109, 1983.

851 [38] R. Peek and W. H. Yi. Error analysis for pseudodynamic test method: 1. Analysis.
852 *Journal of Engineering Mechanics*, 116:1618–1637, 1990.

853 [39] Georges Magonette. Development and application of large-scale continuous pseudo-
854 dynamic testing techniques. *Philosophical Transactions of the Royal Society A Mathematical,
855 Physical and Engineering Sciences*, 359(1786):1771–1799, 2001.

856 [40] Gilberto Mosqueda, Bozidar Stojadinovic, and Stephan A. Mahin. Geographically dis-
857 tributed continuous hybrid simulation. In *13th World Conference on Earthquake Engi-
858 neering*, number 0959, Vancouver, 2004.

859 [41] Oh-Sung Kwon. Multi-platform Hybrid (Experiment-Analysis) Simulations. In *Dynamic
860 Response of Infrastructure to Environmentally Induced Loads*, pages 37–63. Springer, 2017.
861 doi: https://doi.org/10.1007/978-3-319-56136-3__3.

862 [42] Christopher R. Thewalt and Stephen A. Mahin. Non-planar pseudodynamic testing.
863 *Earthquake Engineering & Structural Dynamics*, 24(5):733–746, 1995. ISSN 10969845.
864 doi: 10.1002/eqe.4290240509.

865 [43] F. Javier Molina, G. Verzeletti, G. Magonette, Ph Buchet, and M. Gérardin. Bi-
866 directional pseudodynamic test of a full-size three-storey building. *Earthquake En-
867 gineering and Structural Dynamics*, 28(12):1541–1566, 1999. ISSN 00988847. doi:
868 10.1002/(SICI)1096-9845(199912)28:12<1541::AID-EQE880>3.0.CO;2-R.

869 [44] Oya Mercan, James M. Ricles, Richard Sause, and Thomas Marullo. Kinematic transfor-
870 mations for planar multi-directional pseudodynamic testing. *Earthquake Engineering &*
871 *Structural Dynamics*, 38:1093–1119, 2009. doi: 10.1002/eqe.886.

872 [45] Hussam N Mahmoud, Amr S Elnashai, Billie F Spencer, Jr., Oh-Sung Kwon,
873 and David J Bennier. Hybrid Simulation for Earthquake Response of Semi-
874 rigid Partial-Strength Steel Frames. *Journal of Structural Engineering*, 139(7):
875 1134–1148, 7 2013. ISSN 0733-9445. doi: 10.1061/(ASCE)ST.1943-541X.0000721.
876 URL [http://ascelibrary.org/doi/10.1061/\(ASCE\)ST.1943-541X.0000721](http://ascelibrary.org/doi/10.1061/(ASCE)ST.1943-541X.0000721)
877 <http://ascelibrary.org/doi/10.1061/%28ASCE%29ST.1943-541X.0000721>.

878 [46] Narutoshi Nakata, Erin Krug, and Aaron King. Experimental implementation and verifi-
879 cation of mDOF effective force testing. *Earthquake Engineering & Structural Dynamics*,
880 43:413–428, 2014.

881 [47] Lung-Wen Tsai. *Robot Analysis: The Mechanics of Serial and Parallel Manipulators*.
882 Wiley-Interscience, 1999.

883 [48] Tao Wang, Chun Cheng, and Xun Guo. Model-based predicting and correcting algorithms
884 for substructure online hybrid tests. *Earthquake Engineering & Structural Dynamics*, 41:
885 2331–2349, 2012. doi: 10.1002/eqe.2190.

886 [49] Peng Pan, Gang Zhao, Xinzhen Lu, and Kailai Deng. Force–displacement mixed control
887 for collapse tests of multistory buildings using quasi-static loading systems. *Earthquake
888 Engineering & Structural Dynamics*, 43:287–300, 2014.

889 [50] Guoshan Xu, Zhen Wang, Bin Wu, Oreste S. Bursi, Xiaojing Tan, Qingbo Yang, and
890 Long Wen. Seismic performance of precast shear wall with sleeves connection based on
891 experimental and numerical studies. *Engineering Structures*, 150:346–358, 2017. ISSN
892 18737323. doi: 10.1016/j.engstruct.2017.06.026. URL <http://dx.doi.org/10.1016/j.engstruct.2017.06.026>.

893 [51] Huimeng Zhou, Tao Wang, Chunbo Du, and Cheng Chen. Multi-degree-of-freedom force-
894 displacement mixed control strategy for structural testing. *Earthquake Engineering &
895 Structural Dynamics*, (July):eqe.3334, 8 2020. ISSN 0098-8847. doi: 10.1002/eqe.3334.
896 URL <https://onlinelibrary.wiley.com/doi/abs/10.1002/eqe.3334>.

898 [52] Narutoshi Nakata, Billie F Spencer, Jr., and Amr S Elnashai. Sensitivity-Based External
899 Calibration of Multiaxial Loading System. *Journal of Engineering Mechanics*, 136(2):
900 189–198, 2010. ISSN 0733-9399. doi: 10.1061/(ASCE)0733-9399(2010)136:2(189).
901 URL [http://dx.doi.org/10.1061/\(ASCE\)0733-9399\(2010\)136:2\(189\)http://ascelibrary.org.proxy2.library.illinois.edu/doi/abs/10.1061/\(ASCE\)0733-9399\(2010\)136:2\(189\)http://ascelibrary.org.proxy2.library.illinois.edu/doi/pdf/10.1061/\(ASCE\)0733-9399\(2010\)136:2\(189\)](http://dx.doi.org/10.1061/(ASCE)0733-9399(2010)136:2(189)http://ascelibrary.org.proxy2.library.illinois.edu/doi/abs/10.1061/(ASCE)0733-9399(2010)136:2(189)http://ascelibrary.org.proxy2.library.illinois.edu/doi/pdf/10.1061/(ASCE)0733-9399(2010)136:2(189)).

905 [53] A Blakeborough, M S Williams, A P Darby, and D M Williams. The development
906 of real-time substructure testing. *Philosophical Transactions of the Royal
907 Society of London A: Mathematical, Physical and Engineering Sciences*, 359(1786):
908 1869–1891, 9 2001. ISSN 1364-503X, 1471-2962. doi: 10.1098/rsta.2001.0877.
909 URL <http://rsta.royalsocietypublishing.org/content/359/1786/1869http://rsta.royalsocietypublishing.org/content/roypta/359/1786/1869.full.pdf>.

911 [54] A P Darby, M S Williams, and A Blakeborough. Stability and delay compensation for
912 real-time substructure testing. *Journal of Engineering Mechanics*, 128(12):1276–1284,
913 2002. ISSN 0733-9399. doi: 10.1061/(ASCE)0733-9399(2002)128:12(1276). URL <http://opus.bath.ac.uk/742/>.

915 [55] M I Wallace, D J Wagg, and S A Neild. An adaptive polynomial based forward
916 prediction algorithm for multi-actuator real-time dynamic substructuring. *Proceedings of the Royal Society A: Mathematical, Physical and Engineering Sciences*,
917 461(2064):3807–3826, 12 2005. ISSN 1364-5021. doi: 10.1098/rspa.2005.1532.
919 URL <http://rspa.royalsocietypublishing.org/content/461/2064/3807http://rspa.royalsocietypublishing.org/content/461/2064/3807.full.pdfhttp://rspa.royalsocietypublishing.org/cgi/doi/10.1098/rspa.2005.1532>.

922 [56] Paul A Bonnet, C N Lim, M S Williams, A Blakeborough, S A Neild, D P
923 Stoten, and C A Taylor. Real-time hybrid experiments with Newmark integration,
924 MCSmd outer-loop control and multi-tasking strategies. *Earthquake Engineering &
925 Structural Dynamics*, 36(1):119–141, 1 2007. ISSN 00988847. doi: 10.1002/eqe.
926 628. URL <http://onlinelibrary.wiley.com/doi/10.1002/eqe.628/abstracthttp://doi.wiley.com/10.1002/eqe.628>.

928 [57] Rae-young Jung, P Benson Shing, Eric Stauffer, and Bradford Thoen. Performance of a
929 real-time pseudodynamic test system considering nonlinear structural response. *Earth-*
930 *quake Engineering and Structural Dynamics*, 36(12):1785–1809, 2007. doi: 10.1002/eqe.

931 [58] Cheng Chen, James M Ricles, Ian C Hodgson, and Richard Sause. Real-Time Multi-
932 Directional Hybrid Simulation of Building Piping Systems. In *The 14th World Conference*
933 *on Earthquake Engineering*, pages Beijing, China, 2008.

934 [59] Yunbyeong Chae, James M Ricles, and Richard Sause. Large-scale real-
935 time hybrid simulation of a three-story steel frame building with magneto-
936 rheological dampers. *Earthquake Engineering & Structural Dynamics*, 139
937 (7):1215–1226, 4 2014. ISSN 1096-9845. doi: 10.1002/eqe.2429. URL
938 <http://onlinelibrary.wiley.com/doi/10.1002/eqe.2429/abstract>
939 <http://onlinelibrary.wiley.com/doi/10.1002/eqe.2429/abstract?campaign=woletoc>.

940 [60] Amirali Najafi, Gaston A Fernandois, and Billie F Spencer. Decoupled model-
941 based real-time hybrid simulation with multi-axial load and boundary condition boxes.
942 *Engineering Structures*, 219(October 2019):110868, 9 2020. ISSN 01410296. doi:
943 10.1016/j.engstruct.2020.110868. URL <https://linkinghub.elsevier.com/retrieve/pii/S0141029619344219>.

944 [61] Brian M Phillips and Billie F Spencer, Jr. Model-Based Multiactuator Control
945 for Real-Time Hybrid Simulation. *Journal of Engineering Mechanics*, 139(2):219–
946 228, 2013. ISSN 0733-9399. doi: 10.1061/(ASCE)EM.1943-7889.0000493. URL
947 [http://dx.doi.org/10.1061/\(ASCE\)EM.1943-7889.0000493](http://dx.doi.org/10.1061/(ASCE)EM.1943-7889.0000493)
948 [http://ascelibrary.org/doi/10.1061/\(ASCE\)EM.1943-7889.0000493](http://ascelibrary.org/doi/10.1061/(ASCE)EM.1943-7889.0000493)
949 [http://ascelibrary.org/doi/pdf/10.1061/\(ASCE\)EM.1943-7889.0000493](http://ascelibrary.org/doi/pdf/10.1061/(ASCE)EM.1943-7889.0000493).

950 [62] Xiuyu Gao, Nestor Castaneda, and Shirley J Dyke. Experimental Validation of a
951 Generalized Procedure for MDOF Real-Time Hybrid Simulation. *Journal of Engi-*
952 *neering Mechanics*, 140(4):4013006, 4 2014. ISSN 0733-9399. doi: 10.1061/(ASCE)
953 EM.1943-7889.0000696. URL <http://ascelibrary.org/doi/10.1061/%28ASCE%29EM.1943-7889.0000696>.

954 [63] Gaston A Fernandois and Billie F Spencer. Model-based framework for multi-axial real-
955 time hybrid simulation testing. *Earthquake Engineering and Engineering Vibration*, 16

958 (4):671–691, 10 2017. ISSN 1671-3664. doi: 10.1007/s11803-017-0407-8. URL <http://link.springer.com/10.1007/s11803-017-0407-8>.

959

960 [64] Narutoshi Nakata. Acceleration trajectory tracking control for earthquake sim-
961 ulators. *Engineering Structures*, 32(8):2229–2236, 8 2010. ISSN 01410296. doi:
962 10.1016/j.engstruct.2010.03.025. URL <http://www.sciencedirect.com/science/article/pii/S0141029610001203https://linkinghub.elsevier.com/retrieve/pii/S0141029610001203>.

963

964

965 [65] Ruiyang Zhang, Brian M Phillips, Shun Taniguchi, Masahiro Ikenaga, and Kohju Ik-
966 ago. Shake table real-time hybrid simulation techniques for the performance evaluation
967 of buildings with inter-story isolation. *Structural Control and Health Monitoring*, 24(10):
968 1–19, 2017. ISSN 15452263. doi: 10.1002/stc.1971.

969

970

971 [66] Amirali Najafi and Billie F Spencer, Jr. Validation of Model-Based Real-Time Hybrid
972 Simulation for Lightly-Damped and Highly-Nonlinear Structural System. *Journal of Ap-
973 plied and Computational Mechanics*, 2020.

974

975 [67] Amin Maghreh, Shirley Dyke, Siamak Rabieniaharatbar, and Arun Prakash. Predictive
976 stability indicator: a novel approach to configuring a real-time hybrid simulation. *Earth-
977 quake Engineering & Structural Dynamics*, 46(1):95–116, 2017. doi: <https://doi.org/10.1002/eqe.2775>. URL <https://onlinelibrary.wiley.com/doi/abs/10.1002/eqe.2775>.

978

979 [68] Rui M. Botelho, Xiuyu Gao, Muammer Avci, and Richard Christenson. A robust stability
980 and performance analysis method for multi-actuator real-time hybrid simulation. *Struc-
981 tural Control and Health Monitoring*, page e3017, 2022. doi: <https://doi.org/10.1002/stc.3017>. URL <https://onlinelibrary.wiley.com/doi/abs/10.1002/stc.3017>.

982

983 [69] Geir E. Dullerud and Fernando Paganini. *A Course in Robust Control Theory - A Convex
984 Approach*. Springer, 2000. ISBN 9781475732900.

985 [70] Ning Li, Zihao Zhou, and Zhong-Xian Li. Stability prediction for real-time hybrid
986 simulation with different physical and numerical substructure discretization using asyn-
987 chronous multirate simulation. *Journal of Engineering Mechanics*, 147(11), 2021. doi:
988 10.1061/(ASCE)EM.1943-7889.0001992.

986 [71] L Liqiao, W Jinting, D Hao, and Z Fei. Theoretical and experimental studies on crit-
987 ical time delay of multi-DOF real-time hybrid simulation. *Earthquake Engineering and*
988 *Engineering Vibration*, 21:117–134, 2022. doi: 10.1007/s11803-021-2073-0.

989 [72] G.Y. Liu and S.Y. Chang. Bi-axial pseudodynamic testing. *Proceedings, 12th World*
990 *Conference on Earthquake Engineering, New Zealand*, (1):1–8, 2000. URL <http://www.iitk.ac.in/nicee/wcee/article/0151.pdf>.

991 [73] Chia Ming Chang, Thomas M. Frankie, Billie F. Spencer, and Daniel A. Kuchma. Multiple
992 degrees of freedom positioning correction for hybrid simulation. *Journal of Earthquake*
993 *Engineering*, 19(2):277–296, 2014. ISSN 13632469. doi: 10.1080/13632469.2014.962670.
994 URL <http://dx.doi.org/10.1080/13632469.2014.962670>.

995 [74] Chia-Ming Chang, Thomas M. Frankie, Billie F. Spencer, and Daniel A. Kuchma. Multi-
996 ple Degrees of Freedom Positioning Correction for Hybrid Simulation. *Journal of Earth-*
997 *quake Engineering*, 19(2):277–296, feb 2015. ISSN 1363-2469. doi: 10.1080/13632469.
998 2014.962670. URL <http://www.tandfonline.com/doi/full/10.1080/13632469.2014.962670>.

999 [75] Jamin Park, Raymond Ma, and Oh-Sung Kwon. Model-based adaptive kinematic trans-
1000 formation method for accurate control of multi-DOF boundary conditions in conven-
1001 tional tests and hybrid simulations. *Earthquake Engineering & Structural Dynamics*,
1002 51(5):1076–1095, apr 2022. ISSN 0098-8847. doi: 10.1002/eqe.3605. URL <https://onlinelibrary.wiley.com/doi/10.1002/eqe.3605>.

1003 [76] Nobuyuki Ogawa, Keiichi Ohtani, Tsuneo Katayama, and Heki Shibata. Construction
1004 of a three-dimensional , large-scale shaking table and development of core technology.
1005 *Philosophical Transactions of the Royal Society A Mathematical, Physical and Engineering*
1006 *Sciences*, 359:1725–1751, 2001.

1007 [77] Keiichi Ohtani, Nobuyuki Ogawa, Tsuneo Katayama, and Heki Shibata. Construction
1008 of E-Defense (3-D Full-scale Earthquake Testing Facility). In *13th World Conference on*
1009 *Earthquake Engineering*, page Paper No. 1989, Vancouver, 2004.

1010 [78] Liao Shouqin. ianjin university to take lead in building world’s largest earthquake en-
1011 gineering simulation research facility. <http://www.tju.edu.cn/english/info/1012/1122.htm>, 2022. Accessed: 2020-05-19.

1012

1013

1014

1015

1016 [79] J E Luco, O Ozcelik, and J P Conte. Acceleration Tracking Performance of the UCSD-
1017 NEES. *Journal of Structural Engineering*, (May):481–490, 2010.

1018 [80] Lelli Van Den Einde, Joel P Conte, José I Restrepo, Ricardo Bustamante, Marty Halvor-
1019 son, Tara C Hutchinson, Chin Ta Lai, Koorosh Lotfizadeh, J Enrique Luco, Machel L
1020 Morrison, Gilberto Mosqueda, Mike Nemeth, Ozgur Ozcelik, Sebastian Restrepo, Andrés
1021 Rodriguez, P Benson Shing, Brad Thoen, and Georgios Tsampras. NHERI@UC San
1022 Diego 6-DOF Large High-Performance Outdoor Shake Table Facility. *Frontiers in Built
1023 Environment*, 6(January):1–21, 2021. ISSN 22973362. doi: 10.3389/fbuil.2020.580333.

1024 [81] Siavash Soroushian, E Maragakis, Arash E Zaghi, Esmaeel Rahmanishamsi, Ahmad M
1025 Itani, and Gokhan Pekcan. Response of a 2-story test-bed structure for the seismic eval-
1026 uation of nonstructural systems. *Earthquake Engineering and Engineering Vibration*, 15
1027 (1):19–29, 2016. ISSN 1993503X. doi: 10.1007/s11803-016-0302-8.

1028 [82] Xiao Yan, Juyun Yuan, Haitao Yu, Antonio Bobet, and Yong Yuan. Multi-point shaking
1029 table test design for long tunnels under non-uniform seismic loading. *Tunnelling and
1030 Underground Space Technology*, 59:114–126, 2016. ISSN 08867798. doi: 10.1016/j.tust.
1031 2016.07.002. URL <http://dx.doi.org/10.1016/j.tust.2016.07.002>.

1032 [83] Bo Song, Fei Zheng, and Yue Li. Study on a simplified calculation method for hydrody-
1033 namic pressure to slender structures under earthquakes. *Journal of Earthquake Engineer-
1034 ing*, 17(5):720–735, 2013. ISSN 13632469. doi: 10.1080/13632469.2013.771592.

1035 [84] Yang Ding, Rui Ma, Yun Dong Shi, and Zhong Xian Li. Underwater shaking table tests
1036 on bridge pier under combined earthquake and wave-current action. *Marine Structures*,
1037 58(September 2017):301–320, 2018. ISSN 09518339. doi: 10.1016/j.marstruc.2017.12.004.
1038 URL <https://doi.org/10.1016/j.marstruc.2017.12.004>.

1039 [85] Liao Shouqin. Tianjin University, 2016. URL <http://www.tju.edu.cn/english/info/1009/1463.htm>.

1040 [86] Amr S Elnashai, Billie F Spencer, Jr., Daniel A Kuchma, Guangqiang Yang, Juan E
1041 Carrion, Quan Gan, and Sung Jig Kim. The Multi-Axial Full-scale Sub-structured
1042 Testing and Simulation (MUST-SIM) Facility at the University of Illinois at Urbana-
1043 Champaign. In *Advances in Earthquake Engineering for Urban Risk Reduction*, pages
1044

1045 245–260. Kluwer Academic Publishers, 2006. doi: 10.1007/1-4020-4571-9{_}16. URL
1046 http://link.springer.com/10.1007/1-4020-4571-9_16.

1047 [87] Bora Gencturk and Farshid Hosseini. Evaluation of reinforced concrete and reinforced
1048 engineered cementitious composite (ECC) members and structures using small-scale test-
1049 ing. *Canadian Journal of Civil Engineering*, 42(3):164–177, 2015. ISSN 12086029. doi:
1050 10.1139/cjce-2013-0445.

1051 [88] Catherine W French, Arturo E Schultz, Jerome F Hajjar, Carol K Shield, Douglas W
1052 Ernie, Robert J Dexter, David H.-C. Du, Steven A Olson, Drew J Daugherty, and Chen P
1053 Wan. Multi-axial subassemblage testing (MAST) system: description and capabilities. In
1054 *13th World Conference on Earthquake Engineering*, number August, Vancouver, 2004.

1055 [89] M J Hashemi, J Wilson, and G Burnett. Mixed-Mode Hybrid Simulation of Large-Scale
1056 Structures through Multi-Axis Substructure Testing (MAST) System. In *Proceedings*
1057 *of the Tenth Pacific Conference on Earthquake Engineering*, number November, Sydney,
1058 2015.

1059 [90] Giuseppe Abbiati, Catherine A Whyte, Vasilis Dertimanis, and Bozidar Stojadinovic.
1060 Hybrid simulation of large-scale structures at ETH Zurich: the new 8-actuator multi-
1061 axial subassemblage testing (MAST) setup. In *16th World Conference on Earthquake
1062 Engineering*, number January, page 712, Santiago, 2017. ISBN 1462715524.

1063 [91] Y. Xiao. Experimental Methods for Seismic Simulation of Structural Columns: State-of-
1064 the-Art Review and Introduction of New Multiuse Structural Testing System. *Journal of
1065 Structural Engineering*, 145(3):1–11, 2019. doi: 10.1061/(ASCE)ST.1943-541X.0002269.

1066 [92] Ali Imanpour, Robert Tremblay, Martin Leclerc, Romain Siguier, Guillaume Toutant,
1067 Yasaman Balazadeh Minouei, and Shawn You. Development and application of multi-axis
1068 hybrid simulation for seismic stability of steel braced frames. *Engineering Structures*, 252
1069 (September 2021):113646, feb 2022. ISSN 01410296. doi: 10.1016/j.engstruct.2021.113646.
1070 URL <https://linkinghub.elsevier.com/retrieve/pii/S0141029621017351>.

1071 [93] Kung-Juin Wang, Ming-Chieh Chuang, Keh-Chyuan Tsai, Chao-Hsien Li, Pu-Yuan Chin,
1072 and Shen-Yuo Chueh. Hybrid testing with model updating on steel panel damper sub-
1073 structures using a multi-axial testing system. *Earthquake Engineering and Structural
1074 Dynamics*, 48:347–365, 2019. doi: 10.1002/eqe.3139.

1075 [94] Evan C Bentz, Frank J Vecchio, and Michael P Collins. Simplified modified compression
1076 field theory for calculating shear strength of reinforced concrete elements. *ACI Structural*
1077 *Journal*, 103(4):614–624, 2006. ISSN 08893241. doi: 10.14359/16438.

1078 [95] Saeid Mojiri, Oh Sung Kwon, and Constantin Christopoulos. Development of a ten-
1079 element hybrid simulation platform and an adjustable yielding brace for performance
1080 evaluation of multi-story braced frames subjected to earthquakes. *Earthquake Engineering*
1081 and *Structural Dynamics*, 48(7):749–771, 2019. ISSN 10969845. doi: 10.1002/eqe.3155.

1082 [96] Saeid Mojiri, Pedram Mortazavi, Oh-Sung Kwon, and Constantin Christopoulos. Seis-
1083 mic response evaluation of a five-story buckling-restrained braced frame using multi-
1084 element pseudo-dynamic hybrid simulations. *Earthquake Engineering & Structural Dy-*
1085 *namics*, 50(12):3243–3265, 2021. doi: <https://doi.org/10.1002/eqe.3508>. URL <https://onlinelibrary.wiley.com/doi/abs/10.1002/eqe.3508>.

1086 [97] Thomas T C Hsu, Abdeldjelil Belarbi, and Xiaobo Pang. A Universal Panel Tester.
1087 *Journal of Testing and Evaluation*, 23(1):41–49, 1995. ISSN 00903973. doi: 10.1520/
1088 *jte10397j*.

1089 [98] Walter Kaufmann, Alexander Beck, Demis Karagiannis, and Dominik Werne. The Large
1090 Universal Shell Element Test LUSET. Technical report, 2009. URL <https://doi.org/10.3929/ethz-a-010025751>.

1091 [99] Anthony J Friedman, Shirley J Dyke, Brian M Phillips, Ryan Ahn, Baiping Dong, Yun-
1092 byeong Chae, Nestor Castaneda, Zhaoshuo Jiang, Jianqiu Zhang, Young-Jin Cha, Ali Ir-
1093 mak Ozdagli, Billie F Spencer, James Ricles, Richard E Christenson, Anil Agrawal,
1094 and Richard Sause. Large-Scale Real-Time Hybrid Simulation for Evaluation of Ad-
1095 vanced Damping System Performance. *Journal of Structural Engineering*, 141(6):4014150,
1096 6 2015. ISSN 0733-9445. doi: 10.1061/(ASCE)ST.1943-541X.0001093. URL <http://ascelibrary.org/doi/10.1061/%28ASCE%29ST.1943-541X.0001093>.

1097 [100] Keh-Chyuan Tsai, Hong-Yuan Wang, Chih-Hong Chen, Gee-Yu Liu, and Kung-Juin
1098 Wang. Substructure Pseudo Dynamic Performance of Hybrid Steel Shear Panels. *Steel*
1099 *structures*, 1:95–103, 2001.

1100 [101] Jamin Park, Elias Strelas, Nikos Stathas, Oh-Sung Kwon, and Stathis Bousias. Appli-
1101 cation of hybrid simulation method for seismic performance evaluation of rc coupling

1105 beams subjected to realistic boundary condition. *Earthquake Engineering & Struc-*

1106 *structural Dynamics*, 50(2):375–393, 2021. doi: <https://doi.org/10.1002/eqe.3335>. URL

1107 <https://onlinelibrary.wiley.com/doi/abs/10.1002/eqe.3335>.

1108 [102] M. Seki, M. Teshigawara, and T. Okada. Simulation of Earthquake Response of Re-

1109 inforced Concrete Building Frame by Computer-Actuator On-Line System. In G. A.

1110 Keramidas and C. A. Brebbia, editors, *Proceedings of the International Conference*, pages

1111 317–328, Washington D.C., 1982. Springer, Berlin, Heidelberg. doi: <https://doi.org/10.1007/978-3-662-11353-0>.

1112

1113 [103] Pui-shum B Shing and Stephen A. Mahin. Experimental error propagation in pseudodynamic testing. Technical Report UCB/EERC-83/12, UC Berkeley, Berkeley, 1983.

1114

1115 [104] S. N. Dermitzakis and Stephen A. Mahin. Development of substructuring techniques for

1116 on-line computer controlled seismic performance testing. Technical report, UC Berkeley,

1117 Berkeley, 1985.

1118

1119 [105] Douglas A. Foutch, Subhash C. Goel, and Charles W. Roeder. Preliminary report on

1120 seismic testing of a full-scale six-story steel building. Technical report, University of

Illinois at Urbana-Champaign, 1987.

1121

1122 [106] A. Igarashi, F. Seible, and G. A. Hegemier. Testing of full scale shear wall structures

1123 under seismic load. In *10th World Conference on Earthquake Engineering*, pages 2653–

2658, Rotterdom, 1992.

1124

1125 [107] Koichi Takanashi, Hidetake Taniguchi, and Hisashi Tanaka. Inelastic response of H shaped

1126 columns to two dimensional earthquake motions. *Bulletin of Earthquake Resistant Structure Research Center*, 13:15–28, 1980.

1127

1128 [108] Narutoshi Nakata, Billie F. Spencer, and Amr S. Elnashai. Multi-Dimensional Hybrid

1129 Simulation Using A Six-Actuator Self-Reaction Loading System. In *14th World Conference on Earthquake Engineering*, number January, Beijing, 2008.

1130

1131 [109] Sung Jig Kim, Curtis J Holub, and Amr S Elnashai. Experimental investigation

1132 of the behavior of RC bridge piers subjected to horizontal and vertical earthquake motion.

1133 *Engineering Structures*, 33(7):2221–2235, 7 2011. ISSN 01410296. doi: [10.1016/j.engstruct.2011.03.013](https://doi.org/10.1016/j.engstruct.2011.03.013). URL <http://linkinghub.elsevier.com/retrieve/>

1134 [pii/S0141029611001453](https://www.sciencedirect.com/science/article/pii/S0141029611001453)
1135 <https://www.sciencedirect.com/science/article/pii/S0141029611001453>.

1136 [110] Laura N Lowes, Dawn E Lehman, Anna C Birely, Daniel A Kuchma, Kenneth P Marley,
1137 and Christopher R Hart. Earthquake response of slender planar concrete walls with
1138 modern detailing. *Engineering Structures*, 43:31–47, 10 2012. ISSN 01410296. doi: 10.
1139 1016/j.engstruct.2012.04.040. URL <http://dx.doi.org/10.1016/j.engstruct.2012.04.040>
1140 <https://linkinghub.elsevier.com/retrieve/pii/S0141029612002350>.

1141 [111] Thomas M Frankie, Adel E Abdelnaby, Pedro Silva, David Sanders, Amr S Elnashai, Billie F Spencer, Jr., Daniel Kuchma, and Chia-Ming Chang. Hybrid Simulation
1142 of Curved Four-Span Bridge: Comparison of Numerical and Hybrid Experimental/Analytical Results and Methods of Numerical Model Calibration. In *ASCE Structures
1143 Congress 2013*, pages 721–732, Reston, VA, 4 2013. ISBN 978-0-7844-1284-8.
1144 doi: 10.1061/9780784412848.064. URL <http://ascelibrary.org/doi/abs/10.1061/9780784412848.064>.
1145
1146
1147

1148 [112] Adel E Abdelnaby, Thomas M Frankie, Amr S Elnashai, Billie F Spencer, Daniel A
1149 Kuchma, Pedro Silva, and Chia-Ming Chang. Numerical and hybrid analysis of a
1150 curved bridge and methods of numerical model calibration. *Engineering Structures*,
1151 70:234–245, 7 2014. ISSN 01410296. doi: 10.1016/j.engstruct.2014.04.009. URL
1152 <http://www.sciencedirect.com/science/article/pii/S0141029614002223>
1153 <http://www.sciencedirect.com/science/article/pii/S0141029614002223/pdfft?md5=e2d71a4bfd092d7e6a4cff945d1fff35&pid=1-s2.0-S0141029614002223-main.pdf>
1154 <https://linkinghub.elsevier.com/retrieve/>.
1155

1156 [113] Justin A Murray and Mehrdad Sasani. Near-collapse response of existing RC building
1157 under severe pulse-type ground motion using hybrid simulation. *Earthquake Engineering
1158 & Structural Dynamics*, 45(7):1109–1127, 2016. doi: 10.1002/eqe.

1159 [114] Riadh Al-Mahaidi, M Javad Hashemi, Robin Kalfat, Graeme Burnett, and
1160 John Wilson. *Multi-axis Substructure Testing System for Hybrid Simulation*.
1161 SpringerBriefs in Applied Sciences and Technology. Springer Singapore, Singapore,
1162 2018. ISBN 978-981-10-5866-0. doi: 10.1007/978-981-10-5867-7. URL

1163 <https://link.springer.com/content/pdf/10.1007/978-981-10-5867-7.pdf> http://link.springer.com/10.1007/978-981-10-5867-7.

1165 [115] M Javad Hashemi, Hing-Ho Tsang, Yassamin Al-Ogaidi, John L Wilson, and Riadh
1166 Al-Mahaidi. Collapse Assessment of Reinforced Concrete Building Columns through
1167 Multi-Axis Hybrid Simulation. *ACI Structural Journal*, 114(2):437–449, 3 2017. ISSN
1168 0889-3241. doi: 10.14359/51689438. URL <http://www.concrete.org/Publications/InternationalConcreteAbstractsPortal.aspx?m=details&i=51689438>.

1170 [116] M. Javad Hashemi, Yassamin Al-Ogaidi, Riadh Al-Mahaidi, Robin Kalfat, Hing-Ho Tsang,
1171 and John L. Wilson. Application of Hybrid Simulation for Collapse Assessment of Post-
1172 Earthquake CFRP-Repaired RC Columns. *Journal of Structural Engineering*, 143(1),
1173 2017. doi: 10.1061/(ASCE)ST.1943-541X.0001629.

1174 [117] Ali Y Al-Attraqchi, M Javad Hashemi, and Riadh Al-Mahaidi. Hybrid simulation of
1175 bridges constructed with concrete-filled steel tube columns subjected to horizontal and
1176 vertical ground motions. *Bulletin of Earthquake Engineering*, 18(9):4453–4480, 7 2020.
1177 ISSN 1570-761X. doi: 10.1007/s10518-020-00871-7. URL <https://doi.org/10.1007/s10518-020-00871-7> http://link.springer.com/10.1007/s10518-020-00871-7.

1179 [118] Andrei M Reinhorn, Mettupalayam V Sivaselvan, and Z Liang. Large scale real time
1180 dynamic hybrid testing technique – shake tables substructure testing. In Yoshito Itoh and
1181 Tetsuhiko Aoki, editors, *The First International Conference on Advances in Experimental*
1182 *Structural Engineering*, Nagoya, Japan, 2005. URL [http://civil.eng.buffalo.edu/\\$~\\$reinhorn/PUBLICATIONS/05-08-19-AESE-Hybridtesting.pdf](http://civil.eng.buffalo.edu/$~$reinhorn/PUBLICATIONS/05-08-19-AESE-Hybridtesting.pdf).

1184 [119] Xiaoyun Shao, Andrei M Reinhorn, and Mettupalayam V Sivaselvan. Real-Time
1185 Hybrid Simulation Using Shake Tables and Dynamic Actuators. *Journal of Structural*
1186 *Engineering*, 137(7):748–760, 7 2011. ISSN 0733-9445. doi: 10.1061/(ASCE)ST.1943-541X.0000314. URL <http://ascelibrary.org/doi/10.1061/%28ASCE%29ST.1943-541X.0000314>.

1189 [120] Yingpeng Tian, Xiaoyun Shao, Huimeng Zhou, and Tao Wang. Advances in Real-Time
1190 Hybrid Testing Technology for Shaking Table Substructure Testing. *Frontiers in Built*
1191 *Environment*, 6(August), 2020. ISSN 22973362. doi: 10.3389/fbuil.2020.00123.

1192 [121] Esteban Villalobos Vega, P S Harvey Jr, J M Ricles, L Cao, and Daleen M Torres Bur-
1193 gros. Multi-Directional Real-Time Hybrid Simulation Study of Rolling Pendulum Isolation
1194 Systems for Seismic Risk Mitigation of Critical Building Contents. In *Proceedings of the*
1195 *2022 International Modal Analysis Conference XL*, 2022.

1196 [122] Baiping Dong, Richard Sause, and James M Ricles. Accurate real-time hybrid earthquake
1197 simulations on large-scale MDOF steel structure with nonlinear viscous dampers. *Earth-
1198 quake Engineering & Structural Dynamics*, 44(12):2035–2055, 9 2015. ISSN 00988847.
1199 doi: 10.1002/eqe.2572. URL <http://doi.wiley.com/10.1002/eqe.2572>.

1200 [123] O Na, S Kim, and S Kim. Multi-Directional Structural Dynamic Test using Optimized
1201 Real-time Hybrid Control System. *Experimental Techniques*, pages 1–12, 2 2014. ISSN
1202 07328818. doi: 10.1111/ext.12080. URL <http://doi.wiley.com/10.1111/ext.12080>.

1203 [124] Amirali Najafi and Billie F. Spencer, Jr. Multi-Axial Real-Time Hybrid Simulation for
1204 Substructuring with Multiple Boundary Points. *In press*, 2021.

1205 [125] J. P. Merlet. Parallel manipulators: state of the art and perspectives. *Advanced Robotics*,
1206 8(6):589–596, 1993. ISSN 15685535. doi: 10.1163/156855394X00275.

1207 [126] E. F. Fichter, D. R. Kerr, and J. Rees-Jones. The Gough-Stewart platform parallel
1208 manipulator: A retrospective appreciation. *Proceedings of the Institution of Mechanical
1209 Engineers, Part C: Journal of Mechanical Engineering Science*, 223(1):243–281, 2009.
1210 ISSN 09544062. doi: 10.1243/09544062JMES1137.

1211 [127] Hosam K. Fathy, Zoran S. Filipi, Jonathan Hagen, and Jeffrey L. Stein. Review of
1212 hardware-in-the-loop simulation and its prospects in the automotive area. *Modeling and
1213 Simulation for Military Applications*, 6228E, 2006. ISSN 0277786X. doi: 10.1117/12.
1214 667794.

1215 [128] R. Isermann, J. Schaffnit, and S. Sinsel. Hardware-in-the-loop simulation for the design
1216 and testing of engine-control systems. *Control Engineering Practice*, 7(5):643–653, 1999.
1217 ISSN 09670661. doi: 10.1016/S0967-0661(98)00205-6.

1218 [129] S. Olma, A. Kohlstedt, P. Traphöner, K. P. Jäker, and A. Trächtler. Substructuring
1219 and Control Strategies for Hardware-in-the-Loop Simulations of Multiaxial Suspension

1220 Test Rigs. *International Federation of Automatic Control*, 49(21):141–148, 2016. ISSN
1221 24058963. doi: 10.1016/j.ifacol.2016.10.533.

1222 [130] Andreas Kohlstedt, Phillip Traphöner, Simon Olma, Karl Peter Jäker, and Ansgar
1223 Trächtler. Fast hybrid position / force control of a parallel kinematic load simulator
1224 for 6-DOF Hardware-in-the-Loop axle tests. *IEEE/ASME International Conference on*
1225 *Advanced Intelligent Mechatronics, AIM*, pages 694–699, 2017. doi: 10.1109/AIM.2017.
1226 8014098.

1227 [131] Kim D. Otten, Dzu K. Le, James C. Akers, and Vicente J. Suarez. Status
1228 and Design Features of the new NASA GRC Mechanical Vibration Fa-
1229 cility (MVF), 2010. URL http://www.teamcorporation.com/images/technical_documents/Presentations/NASA_2010_SCLV_MVF.pdf.

1231 [132] MTS Systems Corporation. MAST (Multi-axial Simulation Table) Systems, 2018. URL
1232 https://www.mts.com/cs/groups/public/documents/library/dev_002251.pdf.

1233 [133] C J Holub. Interaction of variable axial load and shear effects in RC bridges. Technical
1234 report, 2005.

1235 [134] B Theon. Generic kinematic transforms package. *MTS Systems Corporation*, 2013.

1236 [135] C H Ligeikis. Exploring uncertainty in real-time hybrid substructuring. Technical report,
1237 University of Connecticut, 2019.

1238 [136] N Tsokanas. Real-time and stochastic hybrid simulation. Technical report, ETH Zurich,
1239 2021.

1240 [137] Amin Maghreh, Yuguang Fu, Herta Montoya, Johnny Condori, Zixin Wang, Shirley J.
1241 Dyke, and Arturo Montoya. A reflective framework for performance management (reform)
1242 of real-time hybrid simulation. *Frontiers in Built Environment*, 6, 2020. doi: 10.3389/
1243 fbuil.2020.568742.

1244 [138] Jean-Pierre Merlet and Clément Gosselin. Parallel Mechanisms and Robots. In Bruno
1245 Siciliano and Oussama Khatib, editors, *Springer Handbook of Robotics*, chapter 12, pages
1246 269–285. Springer Berlin Heidelberg, Berlin, Heidelberg, 2008. ISBN 978-3-540-30301-5.

1247 [139] A. R. Plummer. A Detailed Dynamic Model of a Six-Axis Shaking Table. *Journal*
1248 *of Earthquake Engineering*, 12(4):631–662, may 2008. ISSN 1363-2469. doi:
1249 10.1080/13632460701457264. URL <http://www.tandfonline.com/doi/full/10.1080/13632460701457264>.

1250

1251 [140] Ozgur Ozcelik, Joel P. Conte, and J. Enrique Luco. Comprehensive mechanics-based
1252 virtual model of NHERI@UCSD shake table—Uniaxial configuration and bare table con-
1253 dition. *Earthquake Engineering & Structural Dynamics*, 50(12):3288–3310, oct 2021. ISSN
1254 0098-8847. doi: 10.1002/eqe.3510. URL <https://onlinelibrary.wiley.com/doi/10.1002/eqe.3510>.

1255

1256 [141] J Condori, A Maghareh, and J Orr. Exploiting Parallel Computing to Control Uncertain
1257 Nonlinear Systems in Real-Time. *Experimental techniques*, 44:735–749, 2020. doi: 10.
1258 1007/s40799-020-00373-w.

1259 [142] Y Duan, J Tao, H Zhang, Wang S, and C Yum. Real-time hybrid simulation based on
1260 vector form intrinsic finite element and field programmable gate array. *Structural Control*
1261 and *Health Monitoring*, 26, 2017. doi: 10.1002/stc.2277.

1262 [143] Mohammed Islmail, Faycal Ikhouane, and Jose Rodellar. The hysteresis bouc-wen model,
1263 a survey. *Archives of Computational Methods in Engineering*, 16:161–188, 2009. doi:
1264 10.1007/s11831-009-9031-8.

1265 [144] M. Amir, K.G. Papakonstantinou, and G.P. Warn. A consistent timoshenko hysteretic
1266 beam finite element model. *International Journal of Non-Linear Mechanics*, 119:103218,
1267 2020. ISSN 0020-7462. doi: <https://doi.org/10.1016/j.ijnonlinmec.2019.07.003>. URL
1268 <https://www.sciencedirect.com/science/article/pii/S0020746219300836>.

1269 [145] M. Amir, K. G. Papakonstantinou, and G. P. Warn. State-space formulation for struc-
1270 tural analysis with coupled degradation-plasticity and geometric nonlinearity. *Journal of*
1271 *Structural Engineering*, 148(4):04022016, 2022.

1272 [146] Christian E. Silva, Daniel Gomez, Amin Maghareh, Shirley J. Dyke, and Billie F. Spencer.
1273 Benchmark control problem for real-time hybrid simulation. *Mechanical Systems and*
1274 *Signal Processing*, 135:106381, 2020. ISSN 0888-3270. doi: <https://doi.org/10.1016/j.ymssp.2019.106381>. URL <https://www.sciencedirect.com/science/article/pii/S0888327019306028>.

1275

1276

1277 [147] W Song, C Sun, Y Zuo, V Jahangiri, Y Lu, and Q Han. Conceptual Study of a Real-Time
1278 Hybrid Simulation Framework for Monopile Offshore Wind Turbines Under Wind and
1279 Wave Loads. *Frontiers in Built Environment*, 6(129), 2020.

1280 [148] M Thys, V Chabaud, T Sauder, L Eliassen, L O Saether, and O B Magnussen. Real-time
1281 hybrid model testing of a semi-submersible 10mw floating wind turbine and advances in
1282 the test method). In *Proceedings of the IOWTC 2018 1st International Offshore Wind*
1283 *Technical Conference*, page Paper No. 1081, San Francisco, 2018.

1284 [149] Teng Wu, Shaopeng Li, and Mettupalayam Sivaselvan. Real-time aerodynamics hybrid
1285 simulation: A novel wind-tunnel model for flexible bridges. *Journal of Engineering Me-*
1286 *chanics*, 145(9):04019061, 2019. doi: 10.1061/(ASCE)EM.1943-7889.0001649.

1287 [150] Catherine A. Whyte, Kevin R. Mackie, and Bozidar Stojadinovic. Hybrid simulation
1288 of thermomechanical structural response. *Journal of Structural Engineering*, 142(2):
1289 04015107, 2016. doi: 10.1061/(ASCE)ST.1943-541X.0001346.

1290 [151] G Abbiati, O S Bursi, B Stojadinovic, N Tondini, and C Whyte. Hybrid simulation
1291 of heat transfer problems in structural applications). In *VI International Conference on*
1292 *Computational Methods for Coupled Problems in Science and Engineering*, pages 254–265,
1293 Sitges, 2015.

1294 [152] S J Dyke, K Marais, I Bilionis, J Werfel, and R Malla. Strategies for the design and oper-
1295 ation of resilient extraterrestrial habitats. Proc. SPIE Smart Structures + Nondestructive
1296 Evaluation Conference, 2021.

1297 [153] A Maghareh, A Lenjani, M Krishnan, S J Dyke, and I Bilionis. Role of Cyber-Physical
1298 Testing in Developing Resilient Extraterrestrial Habitats. Proceedings of the ASCE Earth
1299 and Space Conference, 2021.